Fall 12-18-2015

Squamous Cell Carcinoma Response To Cisplatin Exposure

Khanh V. Luong
University of Nebraska Medical Center

SQUAMOUS CELL CARCINOMA RESPONSE TO CISPLATIN EXPOSURE

By

Khanh V. Luong, D.D.S

A THESIS

Presented to the Faculty of

The University of Nebraska Graduate College

In Partial Fulfillment of the Requirements

For the Degree of Master in Science

Medical Sciences Interdepartmental Area

Graduate Program

Oral Biology

Under the Supervision of Professor Aimin Peng

University of Nebraska Medical Center

Omaha, Nebraska

September, 2015

Advisory committee:

Premaraj Sundaralingam, BDS, MS, PhD Gregory Oakley, PhD

James Wahl, PhD

ACKNOWLEDGEMENTS

There are many people who have helped me bring this project to fruition. Foremost, my advisor, Dr. Aimin Peng, has my deepest gratitude for his expertise, understanding, patience, and assistance in many aspects of writing this thesis. Dr. Peng contributed generous amount of time editing my presentations and thesis. He has been an invaluable mentor who I have enjoyed working with immensely.

The other members of my committee have also have been great help: Dr. Premaraj Sundaralingam, Dr. Gregory Oakley and Dr. James Wahl. Dr. Prem provided guidance and encouragement to work hard and finish the research project early. Dr. Oakley had given insightful comments on each of our committee meetings. Dr. Wahl also gave helpful feedback and kindly allowed us to use the time-lapse microscope. The committee has helped shape this thesis into what it is today.

Thirdly, I would like to thank a wonderful group of people I have met in the lab. Ling Wang provided hands on learning with cell culturing while always making sure the lab runs smoothly, whether keeping the supplies stocked or troubleshooting a technical issue. In addition, I acknowledge Brett Roberts and Nick Eurek for their assistance and expertise in running the Zeiss Microscope. I'm especially grateful to Brett for his friendship and input along the way. Lastly, I would like to thank Laura Fisher, Songli Zhu, Jing Zhao and Dapeng Ren for being great labmates and providing a pleasant working environment.

Furthermore, the friendship and support that UNMC College of Dentistry Orthodontic family provided was appreciated. Our assistants, Judy, Sandie and Alyssa, are always making sure the clinic run efficiently to allow me to concentrate on my research. I would like to also thank my Nebraskan friends for making me feel comfortable and my time in Nebraska a memorable one.

Finally, the biggest thanks to my fiancée, Julia, and my family. I thank Julia so much for her encouragement in finishing this thesis. I cannot wait to start our next journey together! My parents have been the biggest inspiration in my life. Their hard work and dedication are contagious. I am grateful for your unconditional love and support.

TABLE OF CONTENTS

ABSTRACT

SQUAMOUS CELL CARCINOMA RESPOSNE TO CISPLATIN EXPSOURE

Khanh V. Luong, D.D.S

University of Nebraska, 2015

Advisor: Aimin Peng, Ph.D.

Purpose: This thesis attempted to quantitatively analyze the individual cell fate choice in resistant head and neck UM-SCC38 cells exposed to cisplatin using the most current techniques available.

Methods: UM-SCC-38 cells were grown in Dulbecco's modified Eagle's medium (DMEM) supplemented with 10% fetal bovine serum (FBS). They were treated with cisplatin and ATM/ATR inhibitors of known dosages. Using live cell imaging, one hundred cells were tracked in each experiment and their behaviors were analyzed and entered into Microsoft Excel Spreadsheet to generate cell profile graphs. HaCaT cells, non-tumorigenic keratinocyte cell line, were also analyzed using live cell imaging and their cell fate profiles generated to better understand the resistance of SCC-38 to cisplatin.

Results: Our study revealed a highly heterogeneous pattern of cell fate choices in SCC-38, in comparison to that of the control, HaCaT, cells. In both SCC-38 and HaCaT cell lines, the majority of cell death occurred in the immediate interphase without mitotic entry, whereas significant portions of SCC-38 cells survived the treatment via either checkpoint arrest or checkpoint slippage. Cells that exhibited checkpoint slippage were primarily treated or

exposed to cisplatin at late-S and G2 phases. Our study also revealed cells in M-phase were hypersensitive to cisplatin. Moreover, although the cisplatin resistant progression of mitosis exhibited no delay in general, greatly prolonged mitosis correlated with the induction of cell death in mitosis. This finding suggested a combinatorial treatment using cisplatin and an agent that blocks mitotic exit, Mg-132. Consistently, we showed a strong synergy between cisplatin and the proteasome inhibitor Mg-132. Finally, targeting DNA damage checkpoint using ATR inhibitor effectively sensitized SCC-38 to cisplatin treatment. To our surprise, targeting checkpoint eliminated both checkpoint arrest and checkpoint slippage, and augmented the induction of cell death in interphase without mitotic entry.

Conclusion: The diverse cell fate choices of SCC-38 and HaCaT cells were confirmed using live cell imaging. Our results showed the majority of cell death occurred in interphase without mitotic entry and a significantly smaller portion of SCC-38 cells died after the cisplatin treatment when compared to HaCaT. On the other hand, analysis of the surviving SCC-38 cells revealed the co-existence of checkpoint arrest and checkpoint slippage. However, caffeine was shown to abolish these surviving mechanisms in cisplatin treated cells. Moreover, our combination therapy of cisplatin plus MG-132 showed strong synergistic effect on SCC-38 cell death. Overall, our study revealed new insights into chemoresistance and suggested combinatorial strategies that potentially overcome cancer resistance.

LIST OF FIGURES

LIST OF TABLES

CHAPTER 1: INTRODUCTION

Squamous cell carcinoma (SCC) of the head and neck is the sixth most common malignancy in the world today (Lingen et al 2010). The etiology is multi-factorial and site-specific. For instance, oral cavity SCC has long been associated with tobacco and alcohol abuse. Despite numerous advances in early cancer detection, prevention, and treatment, the overall 5-year survival remains modest at best (Lingen et al 2010).

At the molecular level, cancer is characterized as genetic alterations to individual cells, leading to cellular functions such as resistance to cell death, increased cell proliferation, and the ability to invade and metastasize (Teng 2015). To combat such tumorigenic cellular behaviors, genotoxic agents are designed to induce apoptosis and other cell death pathways by causing DNA damage (Jackson, 2009). Cancer cells can be particularly vulnerable to DNA damage as they actively undergo DNA replication and cell proliferation. However, the therapeutic benefit of chemotherapy is limited in many clinical cases due to intrinsic or acquired resistance of tumor cells to DNA damage. Thus, it has been suggested that targeting the cellular DNA damage response (DDR) may offer a valuable tool to improve the therapeutic window and effectiveness of chemotherapy (Bolderson et al 2009, Al-Ejeh et al 2010).

Among the most successful and commonly used chemotherapeutic drugs are cisplatin (cis-diamminedichloroplatinum) and other platinum-based drugs. Cisplatin was first approved by the FDA in 1978 for the treatment of testicular

and bladder cancer (Galluzzi et al 2011). Over the past decades, cisplatin and its variants have been prescribed for an estimated 10 to 20 percent of all cancer patients. The use of cisplatin in the treatment of testicular cancer improved the cure rate from 10% to 80%. Today, cisplatin is broadly used for a wide range of other solid tumors, including those of lung, breast, ovarian, head and neck, etc. However, the efficacy of cisplatin in these other solid tumors appears less satisfactory, as many tumors either exhibit intrinsic resistance to cisplatin or relapse despite initial response (Galluzzi et al 2011, Caponigro et al 2006).

Like other genotoxic drugs or radiation, cisplatin exerts cytotoxicity by inducing DNA damage. Specifically, cisplatin binds DNA and cause DNA inter- or intra-strand crosslinking, a form of DNA damage that blocks DNA replication and transcription (Galluzzi et al 2011, Caponigro et al 2006). The occurrence of DNA damage quickly activates the DDR, a conserved mechanism evolved in eukaryotic cells to govern genomic integrity. The DDR encompasses various lesion specific DNA repair pathways, and a sophisticated signaling network that activates the cell cycle checkpoint and cell death (Zhou 2000, Jackson 2009). At the center of the molecular pathway of the DDR are the phosphoinositide 3-kinase-related kinases (PIKK) ATM and ATR. Activation of ATM and ATR by DNA damage in turn results in phosphorylation of dozens of physiological substrates that control various pathways including DNA repair, checkpoint control, and apoptosis (Shiloh 2003). For example, ATM and ATR activate the checkpoint kinases Chk1 and Chk2, which phosphorylate and inactivate Cdc25,

an activator of cyclin-dependent kinases (Cdks), and thereby preventing Cdk activation and cell cycle progression (Sancar et al 2004).

The ultimate result of the DDR can be either cell survival or cell death, and the choice between them may essentially dictate the outcome of cancer therapy. In fact, several distinct cell fate choices should be considered. First, cell death can be induced as the desired outcome that leads to therapeutic benefit. Alternatively, the cell may cease proliferation via sustained activation of the DNA damage checkpoint, a state described as senescence. Although this cell fate choice halts the growth of tumor cells, these cells may re-enter the cell cycle progression after acquiring additional changes. Finally, and perhaps of the worst possibility, cancer cells may continue cell proliferation despite the treatment.

In this study we use automated time-lapse microscopy to quantitate the profile of cell fate determination in resistant cancer cells treated with cisplatin. Our study revealed heterogeneous and complex pattern of cell fate determination in these cancer cells. The results suggested the potential cause of cell protection via both checkpoint activation and checkpoint slippage. More interestingly, our analyses revealed new insights into how targeting mitotic exit and the DNA damage checkpoint can alter the pattern of cell fate choices and enhance the treatment efficacy.

CHAPTER 2: LITERATURE REVIEW

2.1 DNA Damage Response (DDR) Pathways

Each cell in the human body is under constant threat to DNA lesions from both the endogenous and environment agents. The most pervasive environmental DNA-damaging agent is UV light from the sun, which can induce ~100,000 lesions per exposed cell per hour (Jackson 2009). Other common forms of environmental DNA-damaging agent are ionizing radiation and tobacco products. Ionizing radiation can cause double-strand breaks (DSBs), while tobacco products can trigger various cancers, most notably those of the lung and oral cavity (Jackson 2009). Metabolic products such as reactive oxygen species also present challenge to the genomic stability. While the prime objective of each cell is to deliver its genetic material, intact and unchanged, to the next generation, the DNA damage incurred by each cell must be repaired to prevent incorrect transmission of the genetic material. To counter both the endogenous and environmental threats, cells have evolved an intricate series of mechanisms to first, detect DNA damage, second, to accumulate DNA repair factors and third, physically repair the lesion (Zhou 2000). Collectively, these mechanisms are known as the DNA damage response (DDR). In general, DDR can be divided into distinct pathways based on the type of DNA lesion they process. For example, simple DNA changes, such as oxidative lesions and single-strand breaks (SSBs), are repaired through a mechanism called base excision repair (BER); while major mechanisms that cope with double-strand breaks (DSBs) are

homologous recombination and non-homologous end joining (NHEJ) (Lord 2012). The ultimate results of the DDR can either be cell survival or control cell death. If the cell successfully repairs DNA damage, it would turn off the DDR and return to normal cell proliferation; likely wise, if the damage cannot be removed, chronic DDR signaling triggers cell death by apoptosis. However, if the DNA repair mechanism fails, three possible fates are ensured: (1) senescence, (2) apoptosis, and worst of all (3) tumor formation.

2.2 Cisplatin and Its Molecular Mechanisms

Platinum-based drugs are best known for treatment of various solid tumors, including testicular, ovarian, head and neck, colorectal, bladder and lung cancers (Galluzzi et al 2011). *Cis*-diammineplatinum (II) dichloride (best known as cisplatin) was first approved by the FDA in 1978 for the treatment of testicular and bladder cancer (Galluzzi et al 2011). Today, cisplatin is a largely employed platinum-based compound for the treatment of wide spectrum of solid neoplasms, such as testicular, bladder, ovarian, colorectal, lung and head and neck cancers (Toulany et al 2014). Despite positive initial responses, many cancer patients eventually develop chemoresistance to cisplatin-based therapies, leading to relapse and therapeutic failure. High incidence of chemoresistance is cited as the main clinical limitation to the usefulness of cisplatin (Toulany 2014). Therefore, circumventing cisplatin resistance is a critical goal for anticancer therapy and considerable efforts have been undertaken to solve this problem throughout the past decades.

The detailed description of the molecular mechanism of cisplatin can be found elsewhere (Sanderson et al 1996, Siddik 2003). In general, cisplatin exerts its anticancer effects via a complex signaling pathway. Upon cellular absorption and processing, cisplatin must be intracellularly activated by a series of reactions that consist of substituting one or both *cis*-chloro groups with water molecules (Sanderson et al 1996). Equated cisplatin is active and can cause significant damages to both the cytoplasm and nucleus. In the nucleus, cisplatin avidly binds to DNA and causes DNA strand cross-linking. Such distortions in the DNA can be recognized by multiple repair pathways (Siddik 2003). The major signaling network that senses DNA lesion is the DNA damage response (DDR) as discussed above.

2.3 DNA Damage Checkpoints

Cell cycle checkpoints are control mechanisms composed of signaling pathways that control the ability of cells to arrest the cell cycle in response to DNA damage, allowing time for repair. Moreover, it controls the activation of DNA repair pathways and the movement of DNA repair proteins to sites of DNA damage (Zhou 2000).

The recognition of DNA lesions involves the sequential activation of DNA damage sensors, transducers, and effectors. The ataxia telangiectasia mutated (ATM) and RAD3-related protein (ATR) are important sensors of the DNA damage and have been shown to participate in cisplatin-induced DNA damage. Activation of ATM and ATR leads to downstream phosphorylation of various

physiologic substrates (Wang et al 2012). For instance, ATM and ATR activate checkpoint kinase 1 (Chk1, the most prominent substrate and effector of ATR) and checkpoint kinase 2, respectively. Chk1 and Chk2 then phosphorylate and inactivate Cdc25, an activator of cyclin-dependent kinases (Cdks), and thereby preventing Cdk activation and cell cycle progression. In addition, activated ATM and ATR also phosphorylate H2AX at the site of DNA damage, which recruits a number of DDR factors to facilitate DNA repair and checkpoint signaling (Wang et al 2012).

Despite similarity in functions, ATM and ATR are activated through different mechanisms. Mre11-Rad50-Nbs1 complex is the primary sensor of double strand breaks (DSBs). It migrates rapidly to the sites of DMA damage to form nuclear foci and facilitates the recruitment of ATM (Hurley and Bunz 2007). ATR, on the other hand, functions as a sensor for single strand DNA (ssDNA) damage (Hurley and Bunz 2007).

2.4 Caffeine and Its Molecular Mechanism

Caffeine is a popular central nervous system (CNS) stimulant and commonly used as a stimulant to prevent sleepiness. It is found in coffee, tea, cola nuts, and cocoa. For many years, caffeine has been generally believed to suppress cell proliferation, abolish cell cycle progression and enhance the toxicity of radiation and anticancer agents (Bode and Dong 2007). Specifically, caffeine has been reported to induce G1/S arrest and to reverse the G1/S and G2/M checkpoint delay periods. Importantly, when caffeine is combined with DNA-

damaging agents, the potency of the DNA-damaging agent is increased markedly (Bode and Dong 2007). Many studies suggested that the increased toxicity of chemical agents is associated with caffeine's inhibition of the G2 checkpoint activity, which would accelerate movement of the cell cycle through the G2/M checkpoint, thus leaving cells less time to repair DNA damage and eventually lead them to apoptosis.

The cellular effects of caffeine resemble some defects observed in ataxia telangiectasia (AT) cells. Current studies support the evidence that ATM and ATR are primary targets of caffeine (Bode and Dong 2007). ATM and ATR belong to the phosphatidylinositol-3 kinase (PI-3 kinase) and caffeine has been shown to inhibit various forms of PI-3 kinase. Moreover, caffeine also target protein p53, a tumor suppressor protein that is believed to be the primary mediator of cell cycle arrest and induction of apoptosis in most cell lines in response to DNA damage.

2.5 KU55933 and Its Molecular Mechanism

KU-55933 has recently been discovered and is found to have great selectivity for ATM that is 100-fold greater than other related kinases. Studies have shown that KU-55933 induces cell cycle arrest at the G_1 phase and leads to apoptosis under serum starvation conditions (Li and Yang 2010).

2.6 VE-821 and Its Molecular Mechanism

VE-821 is a potent and competitive inhibitor of ATR. Inhibition of ATR led to inhibition of DNA-damage-induced G_2/M arrest in cancer cells. Treatment of cancer cells with anticancer agents along with VE-821 has shown to increase DNA damage and inhibit homologous recombination repair (Prevo et al 2012). This evidence suggests that ATR inhibition with VE-821 is a novel approach to cancer therapy. VE-821 along with cisplatin treatment shows marked synergy (Prevo et al 2012).

2.7 MG-132 and Its Molecular Mechanism

MG-132 is a proteasome inhibitor. It has been shown to inhibit cellular proliferation and induce cell death in esophageal squamous cell carcinoma (Crawford et al 2006). MG-132 induces apoptosis through the activation of class III PI3K pathway and the release of caspase-3.

2.8 UM-SCC-38 Cells

UM-SCC-38 cell line was obtained from Dr. Thomas E. Carey (University of Michigan, Ann Arbor). The cells were originated from a tissue sample of a 60-year-old patient with squamous cell carcinoma of the oropharynx. Previous study by Wang *et al* (2012) showed that among the UM-SCC cell lines, SCC-38 was most resistant to cisplatin. Therefore, we determine it would be most ideal to study the behavior of SCC-38 to cisplatin in adjunct with other agents/inhibitors.

2.9 HaCaT Cells

HaCaT cells are immortalized, non-tumorigenic human keratinocyte. HaCaT cells have been shown to be much more sensitive to cisplatin treatment compared to SCC-38 (Wang et al 2012). For this reason, we will use HaCaT cells as control for our experiment.

CHAPTER 3: MATERIALS AND METHODS

3.1 Cell culture

The oral squamous cell carcinoma cell line, UM-SCC-38, was obtained from Dr. Thomas Carey (University of Michigan, Ann Arbor, MI.) and cells were grown in Dulbecco's modified Eagle's medium (DMEM, Sigma Chemical Co., St. Louis, MO.) supplemented with 10% fetal bovine serum (Hyclone Laboratories, Logan, UT). They were incubated in a humidified atmosphere of 5% CO_2 at 37-^{o}C. HaCat cells were obtained from Dr. Pam Jensen (University of Pennsylvania, Philadelphia, PA.) and were passaged using DMEM medium lacking calcium (Invitrogen, Grand Island, NY.) supplemented with 10% fetal bovine serum. Unless specified, prior to each live cell microscopy cells were transferred to a 6-well plate (CELLTREAT Scientific Products, Shirley, MA) and grown in DMEM medium for 24 hours prior to treating with appropriate drug or inhibitor concentrations.

3.2 Cisplatin preparation

Cisplatin was purchased in powder form, cis-diammineplatinum (II) dichloride (Sigma, St. Louis, MO). Cisplatin has a molecular weight of 300.01 g/mol. The stock solution was prepared in purified water (ddH_2O) to 3 mM and kept in -20^{o}C environment. A new bath of 3 mM stock solution was prepared every 6 months to avoid any potential long-term changes to the structures of the complex. Unless specified, cisplatin was used at a final concentration of 16 µM throughout this entire experiment.

3.3 Inhibitor preparation

The following inhibitors were used: caffeine (Sigma, St. Louis, MO), KU 55933, an ATMi inhibitor (EMD Chemicals), VE-821, an ATRi inhibitor (SELLECK Chemical LLC) and Mg-132, a proteasome inhibitor (Sigma, St. Louis, MO). Caffeine (anhydrous) has a molecular weight of 194.2 g/mol. Caffeine stock solution was prepared in purified water (ddH_2O) to 100 mM. KU 55933, VE-821 and Mg-132 were all purchased in power form and dissolved in DMSO to make a stock solution of 5 mM, 10 mM and 100 mM, respectively. All inhibitors were stored and kept in -20^oC environment. The final concentrations of these inhibitors were obtained from the literatures and they are 4 mM for caffeine, 20 µM for KU-55933, 10 µM for VE-821, and 5 µM for Mg-132 (Ashley et al 2014).

3.4 Pilot study design

3.4.1 Determining the best cisplatin concentration

The purpose of the pilot study was to determine the best dose and timeframe to study cell death. Two days prior to live cell microscopy cells were passaged and seeded in a 24-well plate (CELLTREAT Scientific Products, Shirley, MA) at roughly 50 to 80% confluence. Each well contained 1 mL DMEM and the plate was incubated at 37^oC for 24 hours. On the next day cells were treated at four different cisplatin concentrations: 4 µM, 8 µM, 16 µM, and 32 µM (Fig. 3.4.1). The plate was incubated again for another 24 hours. The following observations were made after 24 hours: almost all cell death were observed in 32 µM wells, minimal to no cell death at 4 µM wells and roughly 50% cell death

observed at 16 µM wells. Therefore, we decided 16 µM cisplatin would be the optimal cisplatin concentration to study cell death.

3.4.2 Does caffeine alone have any effect on cell behavior?

To ensure that caffeine alone does not have significant effect on cell behavior, we performed a pilot study of caffeine treatment. Similar to cisplatin setup above, UM-SCC-38 cells were seeded in a 6-well plate. It was incubated at 37^{o}C for 24 hours. On the second day, only caffeine (4 µM) was added to the experimental well (Figure 3.4.2). However, instead of tracking cell behavior under the time lapse microscope, we incubated the plate again for another 24 hours. The cells were observed under the light microscope and an image was taken to capture the post-caffeine cell population as well as the control group (Figure 4.5.4). Clearly, caffeine alone did not show any significant effect on cell death compared to the control group.

3.5 Time Lapse Experiment and Study Design

3.5.1 Cisplatin Only

One day prior to time lapse microscopy, UM-SCC-38 cells were seeded in a 6-well plate at roughly 80% confluence. Each 35-mm well contained 2.5 mL DMEM solution. The plate was then incubated at 37^{o}C for 24 hours. Twenty-four hours later, cisplatin was added to the experimental well. The control well was imaged without any drug to serve as control. The amount of drug was calculated based on the amount of solution in the well and the desired drug concentration. For example, 16 µM cisplatin in 2.5 mL solution is calculated as follow:

$$amt.\,of\ cisplatin\ needed\ (\mu L) = \frac{16\mu mol}{L}\,x\,\frac{2.5\ ml}{}\,x\,\frac{L}{1000mL}\,x\,\frac{L}{300\mu mol}\,x\,\frac{10^6}{L} = 133.3\mu L$$

$\frac{16\mu mol}{L}$ $= desired\ cisplatin\ concentration$

$2.5\ ml$ $= volume\ in\ each\ well$

$\frac{L}{1000mL}$ $= conversion\ unit$

$\frac{L}{300\mu mol}$ $= concentration\ of\ cisplatin\ stock\ solution$

Unless specified, the amount of cisplatin remained constant through this entire experiment. The plate was then loaded into Zeiss time-lapse microscope for 24-hour imaging. Figure 3.5.1 illustrates cisplatin study design.

3.5.2 Cisplatin and MG-132

All procedures all similar as mentioned above. The design is illustrated in figure 3.5.2. The amount of MG-132 was calculated as follow:

$$amt.\,of\ MG132\ needed\ (\mu L) = \frac{5\mu mol}{L}\,x\,\frac{2.5\ ml}{}\,x\,\frac{L}{1000mL}\,x\,\frac{L}{1000\mu mol}\,x\,\frac{10^6}{L} = 12.5\mu L$$

3.5.3 Cisplatin and Caffeine

The study design for cisplatin and caffeine is illustrated in figure 3.5.3. The amount of caffeine was calculated as follow:

$$amt.\,of\ caffeine\ needed\ (\mu L) = \frac{4mmol}{L}\,x\,\frac{2.5\ ml}{}\,x\,\frac{L}{1000mL}\,x\,\frac{L}{100mmol}\,x\,\frac{10^6}{L} = 100\mu L$$

3.5.4 Cisplatin and ATMi/ATRi

The study design for cisplatin and ATMi/ATRi is illustrated in figure 3.5.4. The amounts of KU-55933 and VE-821 are calculated as follow:

$$amt.\,of\ KU - 55933\ needed\ (\mu L) = \frac{20\mu mol}{L}\,x\,\frac{2.5\ ml}{}\,x\,\frac{L}{500\mu mol}\,x\,\frac{10^6\mu L}{L} = 100\mu L$$

$$amt.\,of\ VE - 821\ needed\ (\mu L) = \frac{10\mu mol}{L}\,x\,\frac{2.5\ ml}{}\,x\,\frac{L}{1000mL}\,x\,\frac{L}{100\mu mol}\,x\,\frac{\text{-}10^6}{L} = 250\mu L$$

3.5.5 Live cell microscopy and cell imaging analysis

Immediately after drug/inhibitor addition, live cell imaging was performed using a Zeiss Microscope with Marianas Software (Intelligent Imaging Innovations, Inc. Denver, CO.), with images collected at 10X objective every 10 minutes for 24 hours. Image sequences were viewed using Slidebook Reader 5.5 (Intelligent Imaging Innovations, Inc. Denver, CO.). Once the live cell microscopy was completed, the captured images were loaded into SlideBook Reader Software (3i, Denver, CO). In each well one hundred cells were tracked for cell fates (Figure 3.5.5).

3.6 Graphs Generation

Cell behaviors were recorded manually and entered into Microsoft Excel Spreadsheet to generate cell profile graphs (Figure 3.6).

3.7 Statistical Analysis

Statistical significance was analyzed using an unpaired 2-tailed Student's t-test. The values are presented as the means ± standard errors. A P-value <0.05 was considered statistically significant.

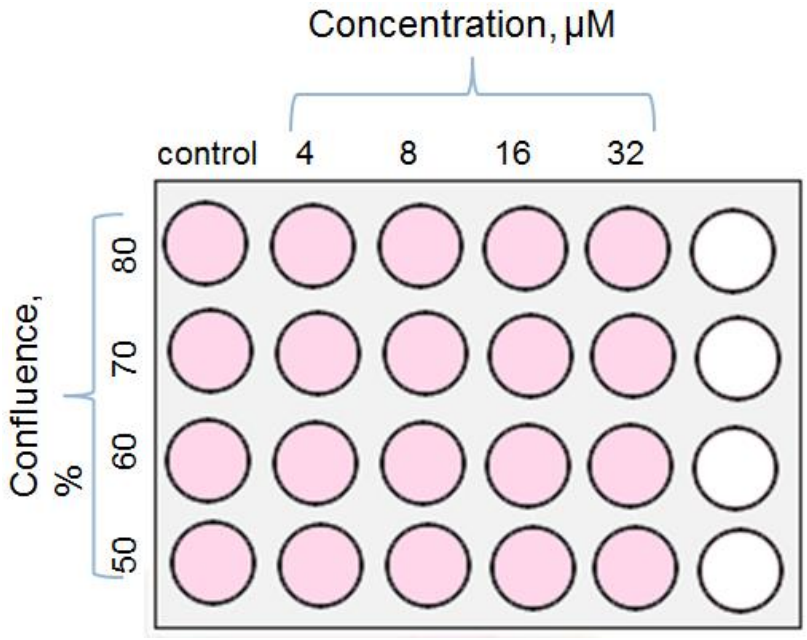

Figure 3.3.1. Pilot study design
SCC-38 cells were treated with 16 different combinations of cisplatin concentration and cellular confluence. Each well contained 1 mL DMEM solution. Left column contained SCC-38 cells without cisplatin treatment to serve as control.

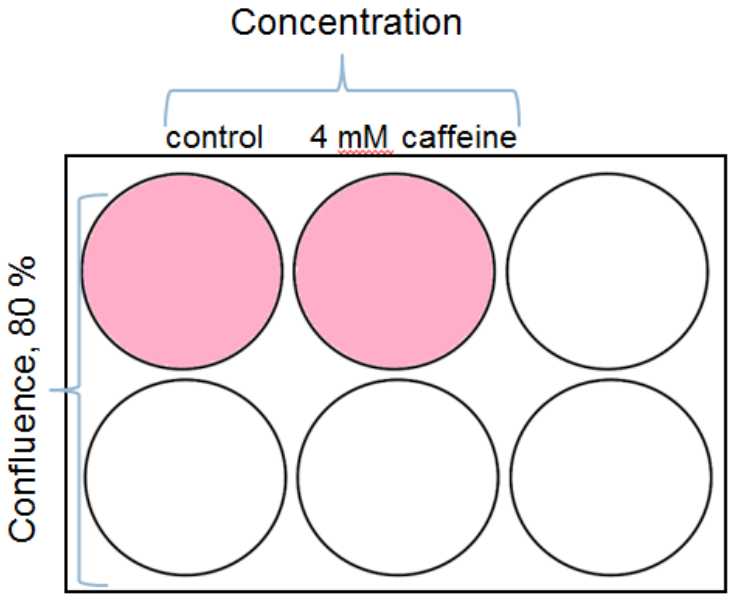

Figure 3.3.2. Caffeine only study design
SCC-38 cells were treated with or without 4 mM caffeine only.

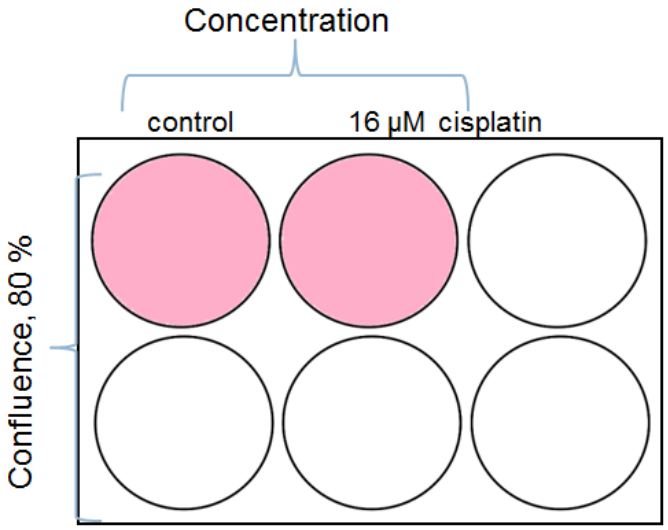

Figure 3.5.1. Preparing for cisplatin time-lapse experiment
SCC-38 cells were seeded in 6-well plate. They were treated with or without 16 µM cisplatin.

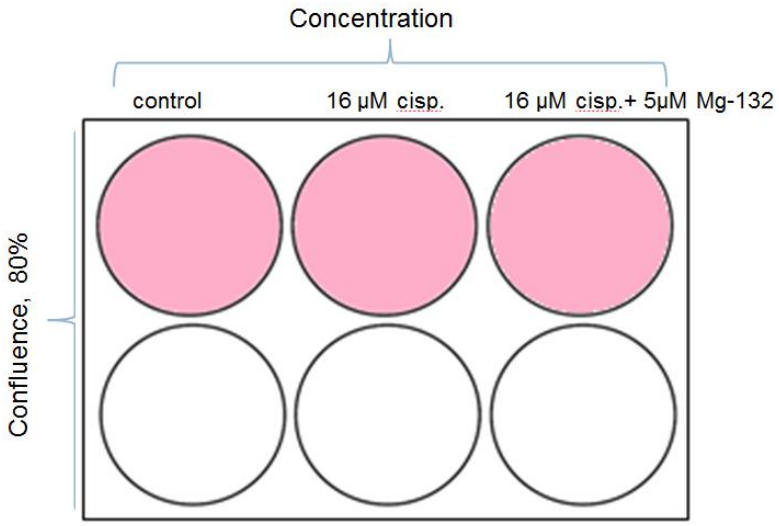

Figure 3.5.2. Preparing for cisplatin-Mg-132 time-lapse experiment
SCC-38 cells were treated with cisplatin alone or cisplatin plus Mg-132 combination.

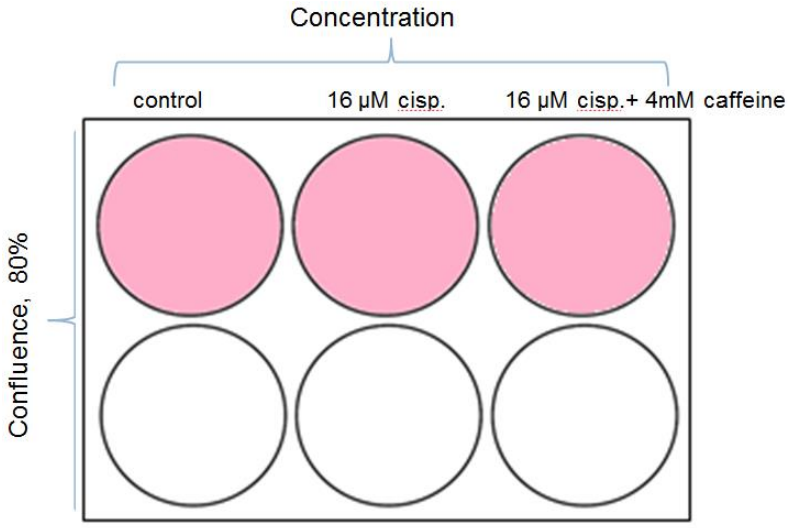

Figure 3.5.3. Preparing for cisplatin-caffeine time-lapse experiment
SCC-38 cells were treated with cisplatin alone or cisplatin plus caffeine combination

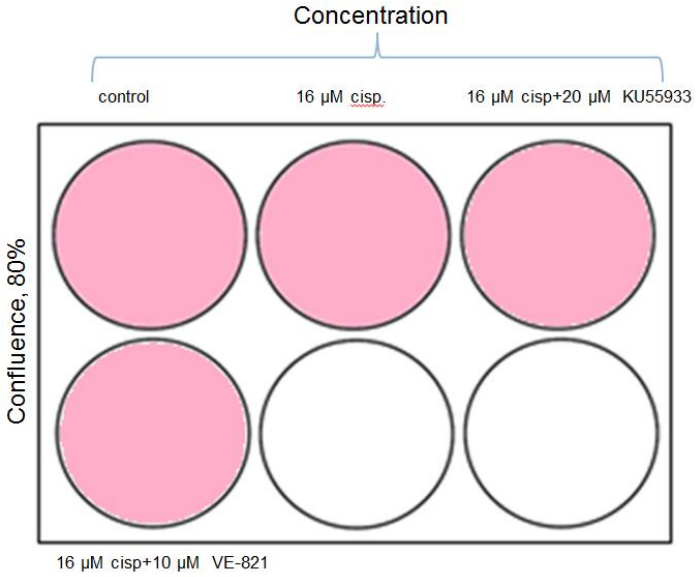

Figure 3.5.4. Preparing for cisplatin-caffeine time-lapse experiment
SCC-38 cells were treated with cisplatin alone, cisplatin-KU55933 or cisplatin-VE-821 combination.

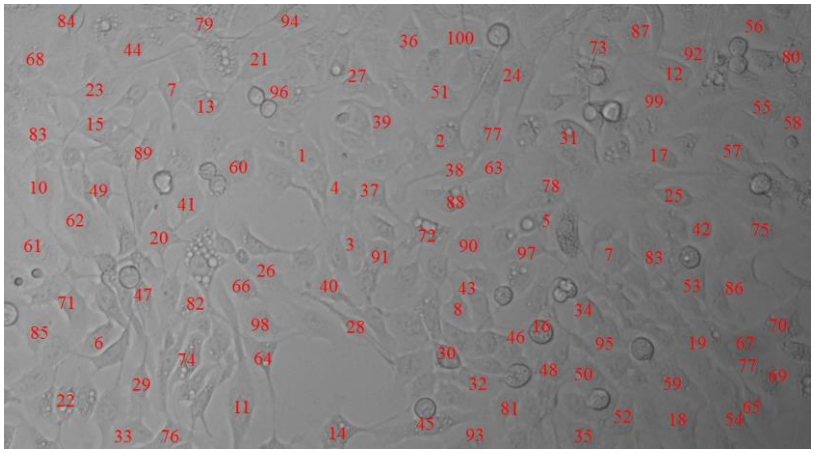

Figure 3.5.5. SCC-38 cell labeling
This image illustrates a time-lapse image with one hundred SCC-38 cells labeled. Each cell was tracked for their behavior during the entire 24-hour experiment.

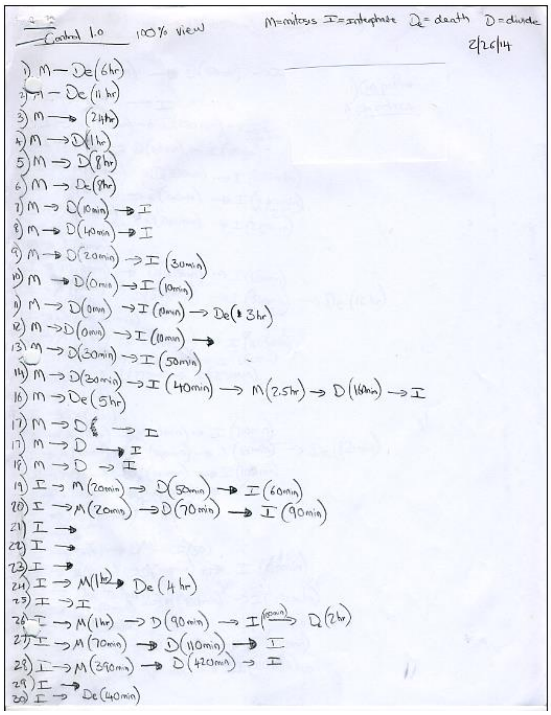

Figure 3.6. Recorded SCC-38 cell behavior
This image provides an example of recorded cell behavior. The data were entered into Microsolf Excel to generate figure profiles.

CHAPTER 4: RESULTS

4.1 Chemoresistant cancer cells display diverse fate profiles

As discussed in our literature review section, SCC-38 cell line was selected because this head and neck squamous cell carcinoma (HNSCC) has been previously characterized to be resistant to cisplatin treatment (Wang et al 2012, Brenner 2010). To shed new light on cisplatin resistance, live cell imaging was utilized to determine the initial fate of UM-SCC38 cells after cisplatin exposure (Fig. 4.1.1, Fig. 4.1.2). Cell profiles from six consecutive experiments show consistent results: the vast majority of unperturbed SCC-38 cells underwent normal cell division, while a dramatically different cell fate profile existed in the presence of cisplatin (Fig. 4.1.3). As expected, a significant induction of cell death was observed in cells exposed to cisplatin, 60% compared to 15% cell death in untreated sample (Table 4.1). Cell death was further investigated for the cell cycle stage in which it occurred. For example, death in interphase defined those cells that died in the immediate interphase without mitotic entry; death in mitosis characterized those that entered mitosis and died during mitosis; and finally, some cells died in the second interphase after mitotic entry and exit. As evident in Figure 4.1.4, the majority of cell death (45%) induced by cisplatin occurred in interphase without mitotic entry. A moderate increase (13%) was documented in cell death in interphase after the first mitosis, but no increase was seen in the portion of mitotic cell death (Fig. 4.1.4). Therefore, although mitotic cell death has been implicated in chemotherapy, e.g.

via mitotic catastrophe, it did not appear to play a significant role in the treatment of cancer cells with cisplatin.

Consistent with the previously characterized chemoresistance of SCC-38 cells, significant portions of cells (40%) survived the treatment. As shown in Figure 4.1.5, cisplatin induced DNA damage checkpoint was evidenced by approximately 25% of cells remained in the interphase throughout the 24-hour period, compared to 2% in the drug-free group. The activation of DNA damage checkpoint after cisplatin treatment was consistent with previous study (Galluzzi et al 2011; Prendergast et al 2011; Pabla et al 2008). Moreover, an average 14% of cells underwent continuous cell cycle progression despite cisplatin treatment. Thus, this portion of cells escaped the induction of cell death and checkpoint arrest (Fig. 4.1.6). This cell fate choice is classified here as “checkpoint slippage”, as also implicated in previous studies (Shaltiel et al 2015, Bartek et al 2007, Clemenson et al 2009, Syljuasen 2007). The nature of checkpoint slippage is not fully understood at the present moment. In principle, the deficiency of checkpoint activation can lead to continued cell division after DNA damage. Alternatively, the checkpoint may be initially activated but de-activated subsequently due to DNA repair, or hyperactivation of checkpoint recovery or adaptation mechanisms (Clemenson et al 2009, Syljuasen 2007, Peng 2013)

Interestingly, cells in the group of checkpoint slippage entered mitosis in approximately 3.5 hours after cisplatin-treatment (Fig. 4.1.7). By comparison, mitotic entry in unperturbed cells took 7 hours in average (Fig. 4.1.7). We speculated that the difference in the timing of mitotic entry reflected a cell cycle-

dependence of checkpoint slippage. For example, cells slipped into mitosis were exposed to cisplatin in late S and G2 phases, whereas cells treated in G1 and early S phases was effectively prevented from mitotic entry due to checkpoint arrest or cell death. There are several possible mechanisms underlying this observation. First, induction of DNA damage by cisplatin may be less efficient in late S and G2 cells, or alternatively, the DNA damage checkpoint in late S and G2 is inadequate in preventing mitotic entry. Notably, previous studies indicated that an imperfect G2/M DNA damage checkpoint failed to halt the cell cycle with a subthreshold level of DNA damage (Deckbar et al 2007; Krempler et al 2007).

4.2 Duration of mitotic arrest does not dictate cell fate

Mitotic arrest can result from erratic progression of mitosis and activation of the mitotic spindle checkpoint. Surprisingly, no mitotic arrest was induced by cisplatin treatment, as cells in the control and cisplatin-treated groups spent similar amount of time in mitosis, 43 minutes and 40 minutes, respectively (Fig. 4.2.1). We further separated the cisplatin-treated and mitotic-entering cells into three groups based on their subsequent cell fate: died in mitosis, exited mitosis and survived, or exited mitosis and died in the following interphase (Fig. 4.2.2). We observed no correlation between mitotic duration and the subsequent cell fate after mitotic exit (Fig. 4.2.2). Therefore, we concluded mitotic duration does not predict cell death or survival in the subsequent interphase. However, dramatically prolonged mitosis was associated with mitotic death, as cells that destined to die in mitosis spent an average of 126 minutes in mitosis before undergoing apoptosis (Fig. 4.2.2). This finding suggested delaying mitotic exit may enhance

the effectiveness of cisplatin by inducing cell death in mitosis. To directly test this hypothesis, we co-treated SCC-38 cells with Mg-132, a proteasome inhibitor known to suppress M-phase exit (Skoufias et al 2007). Very surprisingly, the combination of cisplatin and Mg-132 caused 96% mitotic cell death, compared to less than 4% with cisplatin alone (Fig. 4.2.3). Similarly, the finding was confirmed in Dr. Peng's lab with cell proliferation and clonogenic assays (Fig. 4.2.4, Fig. 4.2.5).

4.3 SCC-38 M-phase cells are hypersensitive to cisplatin

As we understood, cisplatin induced cell death by causing DNA crosslinking, the process that interferes with DNA replication and transcription (Galluzzi et al 2011; Caponigro et al 2006). Moreover, recent studies revealed that mitotic DNA damage responded differently from that of interphase cells; it is often diminished (Heijink et al 2013; Giunta et al 2010). Hence, this knowledge prompted us to examine the fate of cells exposed to cisplatin during mitosis, a cell cycle stage in which DNA replication and transcription are suppressed. Figure 4.3.1 represents a collection of M-phase cells that were exposed to cisplatin from all of our experiments. Similar to interphase cells, M-phase cells exhibited multiple fates following cisplatin exposure (Fig. 4.3.1). However, M-phase cells were extremely sensitive to cisplatin, and the chance of cell survival was markedly reduced in cells exposed to cisplatin in mitosis: 7% survival in M-phase compared to 44% in interphase (Fig. 4.3.2). Of the 93% of M-phase cells died after cisplatin treatment, 34% died during mitosis and the other 59% completed cell division, and then died in the subsequent interphase (Table 4.3). Furthermore, 29% of

cells died in early mitosis prior to any sign of cell division, whereas 5% cells death occurred in late stages of mitosis. In light of these results, we concluded that 1) cisplatin exerted cytotoxicity in mitotic cells independent of DNA replication and transcription, and 2) cisplatin induced cell death in mitotic cells with a much higher potency compared to that in interphase cells.

4.4 Chemoresistant cells are protected from cell death by both checkpoint arrest and slippage

To better understand the cisplatin resistance of SCC-38 cells, we comparatively analyzed the cell fate profile of HaCaT, a spontaneously transformed keratinocyte cell line known to be cisplatin-sensitive (Wang et al 2012). Cell profiles of SCC-38 and HaCaT being treated with cisplatin are shown in Figure 4.4.1. Evidently, marked difference in cell fate profiles was noticed between cisplatin-treated SCC-38 and HaCaT cells. As expected, cisplatin induced cell death more efficiently in HaCaT cells (Fig. 4.4.1). Approximately 88% of HaCaT cells died in interphase compared to 45% of SCC-38 cells (Fig. 4.4.2). By comparison, cell death in mitosis or cell death in interphase after the first mitosis was not increased, but rather moderately reduced in HaCaT cells (Fig. 4.4.2). Importantly, and in sharp contrast to SCC-38 cells, HaCaT cells exhibited much less checkpoint activation and checkpoint slippage in response to cisplatin. Only 4% HaCaT cells remained arrested in interphase in comparison to 28% in SCC-38; and 1% of HaCaT cells underwent continued cell cycle progression in the presence of cisplatin, compared to 11% of SCC-38 cells (Fig. 4.4.3). This

comparative study of cell fate profiles underlied the critical role of both checkpoint activation and slippage in protecting cells from cell death, which may subsequently lead to cancer resistance.

4.5 Caffeine sensitizes cell death by abolishing both checkpoint activation and checkpoint slippage

It has been suggested that targeting the cellular DDR mechanism rendered cell defenseless. We thought this process would make cancer cells more susceptible to radiation and chemotherapy. For example, it is typically thought that disruption of the DNA damage checkpoint will allow cell cycle progression after DNA damage. And subsequently, cell division with unrepaired DNA damage leads to further accumulation of DNA damage, mitotic defects, and eventually, cell death. Our objective was to determine how the checkpoint disruption would affect the determination of cell fate choices in SCC-38 cells treated with cisplatin. First, it was confirmed, with Western blot in Dr. Aimin Peng's lab, that caffeine, a well-characterized inhibitor of ATM and ATR, effectively silenced DNA damage checkpoint signaling induced by cisplatin in SCC-38 cells, as evidenced by impaired phosphorylation of Chk1 and Chk2 (Fig. 4.5.1). We then performed four consecutive time lapse imaging experiments with caffeine and cisplatin treatment and cell profile data show consistent results (Figure 4.5.2). Caffeine plus cisplatin treatment resulted in 88% cell death in interphase, significantly higher than 51% observed in cisplatin only treatment ($P<0.001$,Figure 4.5.3). However, no significant cell death in mitosis or the second interphase following the first mitosis

was observed between the cisplatin only and cisplatin-caffeine treatments (Fig. 4.5.3). This effect of caffeine strongly argued that checkpoint disruption directly sensitizes cell death without either mitotic entry or accumulation of DNA damage due to mitotic defects. To determine how much effect caffeine had on cell behavior alone and to serve as a control, we conducted a pilot study in which SCC-38 cells were treated with the same concentration caffeine (4 mM). As indicated in Figure 4.5.4, caffeine did not induce cell death in SCC-38 cells. We then compared the portions of surviving cells between groups of cisplatin alone and cisplatin/caffeine combination treatment. As expected, caffeine abolished the portion of interphase arrested cells (Fig. 4.5.5), presumably by suppressing the ATM/ATR-mediated DNA damage checkpoint. To our surprise, caffeine treatment also completely eliminated the portion of checkpoint slippage, as essentially no cell was able to successfully complete cell division in the presence of caffeine and cisplatin (Fig. 4.5.5). Collectively, caffeine treated SCC-38 responded to cisplatin in a manner similar to the chemosensitive HaCaT cell. Again, our findings with live cell microscopy were confirmed in Dr. Peng's lab that caffeine greatly enhanced the efficacy of cisplatin in SCC-38 cells using both cell proliferation and clonogenic assays (Fig. 4.5.6, Fig. 4.5.7).

4.6 Inhibition of ATR, but not ATM, sensitizes interphase cell death

Caffeine inhibits both ATM and ATR, the two upstream DDR kinases. It has been well illustrated that ATM and ATR, though sharing great similarity in structural elements and substrate recognition, respond to different types of DNA lesions and are activated by distinct mechanisms (Shiloh 2003). To better understand

the involvement of ATM and ATR in DNA repair mechanism, we utilized specific inhibitors that selectively target either ATM or ATR. As discussed and confirmed previously in Dr. Peng's lab with Western blot, KU-55933 (ATMi) inhibited phosphorylation of Chk2 in response to cisplatin, whereas VE-821 (ATRi) disrupted ATR-dependent phosphorylation of Chk1 (Fig. 4.5.1).

Based on the cell profile data from four consecutive time-lapse microscopy experiments, the results were very consistent (Fig. 4.6.1). ATM inhibition did not significantly alter the profile of cell fate choices after cisplatin treatment (Fig. 4.6.2). For instance, on average 50% of SCC-38 cells treated with cisplatin resulted in cell death in interphase without mitotic entry, while 45% of SCC-38 cells experienced similar fate when exposed to cisplatin-ATMi combination ($P>0.05$). Moreover, 11.8% of SCC-38 cells treated with cisplatin died in the second interphase following the first mitosis, compared to 11.5% of cancer cells underwent similar fate in cisplatin/ATMi combination group ($P>0.05$). Only a moderate induction of mitotic cell death was detected with ATM inhibition ($P=0.03$, Fig. 4.6.2). In addition, we observed no difference between cisplatin only and cisplatin/ATMi treated cells in term of cell survival via interphase arrest (checkpoint activation) or checkpoint slippage (Fig. 4.6.3). ATR, on the other hand, sensitized interphase cell death to approximately 70%, as compared to 50% in the group of cisplatin-treated only group($P=0.03$, Fig. 4.6.2). Moreover, ATR inhibition substantially reduced the number of cells that were arrested in interphase or underwent checkpoint slippage (Fig. 4.6.3). The impact of ATR inhibition on the profile of post-cisplatin cell fate resembled that of caffeine,

suggesting that ATR, rather than ATM, plays a major role in cell fate determination after cisplatin treatment. Our conclusion was later confirmed by the works in Dr. Peng's lab using cell proliferation and clonogenic assays (Fig. 4.6.4, Fig. 4.6.5). Thus, ATR-mediated checkpoint pathway presents a promising target to improve the therapeutic outcome using cisplatin.

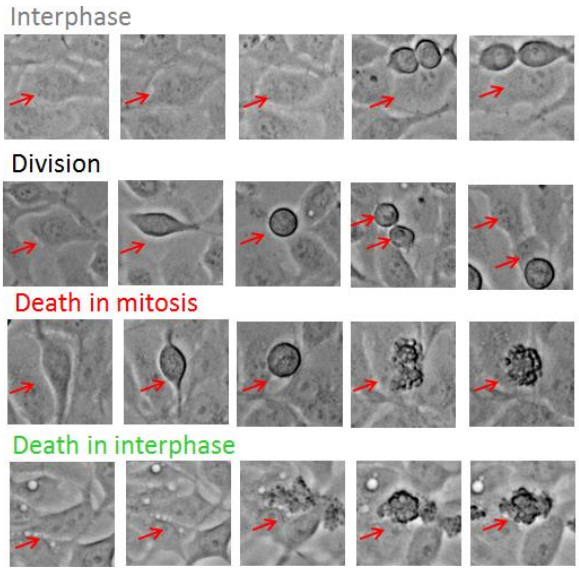

Figure 4.1.1. Time-lapse sequences of SCC-38 cell
This figure illustrates the time-lapse sequences illustrating the fates exhibited by SCC-38 cells following prolonged exposure to cisplatin, 16 µM.
The four main behaviors of SCC-38 cells observed using time-lapse microscope were proliferation in interphase, division, death in mitosis and death in interphase.

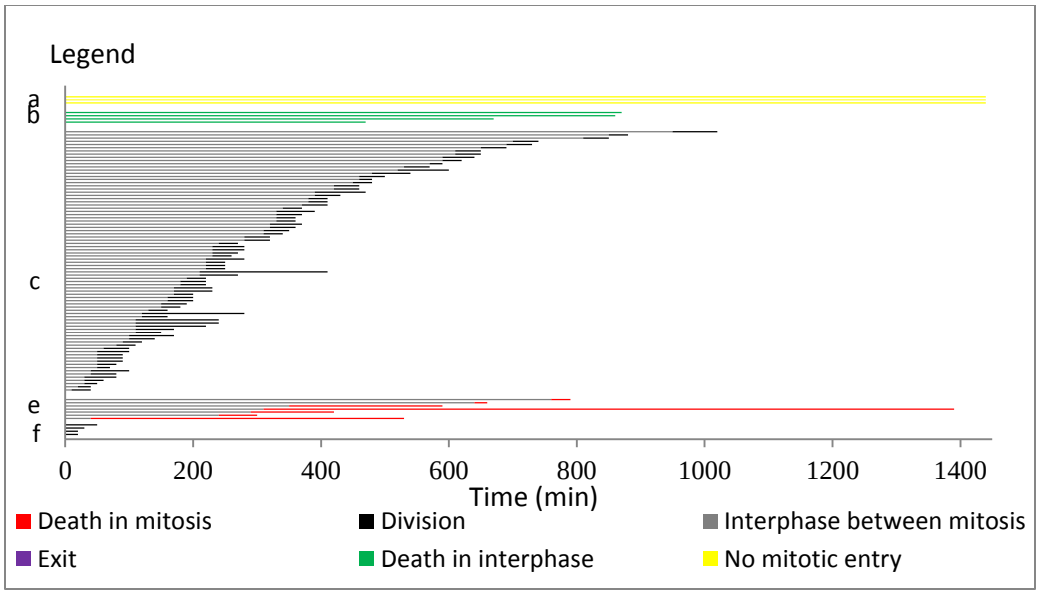

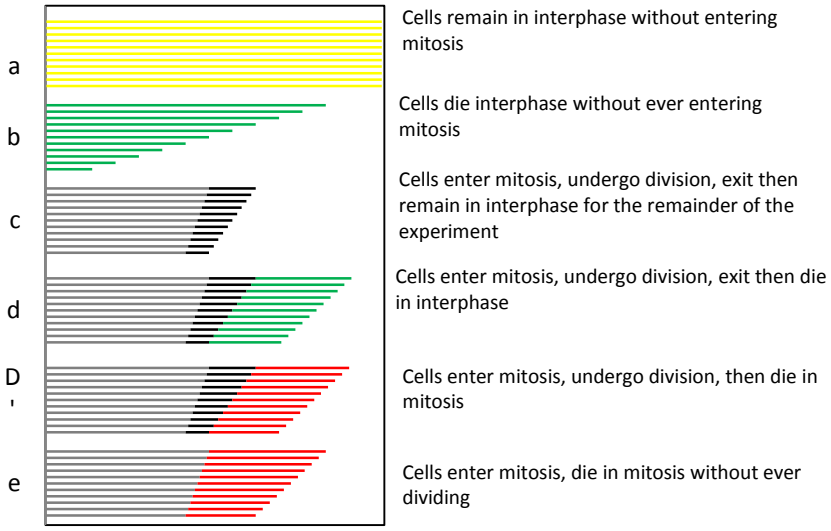

Figure 4.1.2. Profiling the cell fate choices
This figure illustrates how cell profile was constructed. Each horizontal line represents one cell, with the length of the line corresponding to the duration of a given behavior. The color of the line represents cell behavior.
Note, when cells exit mitosis and remain in the interphase for the remainder of the experiment, the line ends when the cell exits mitosis.

.

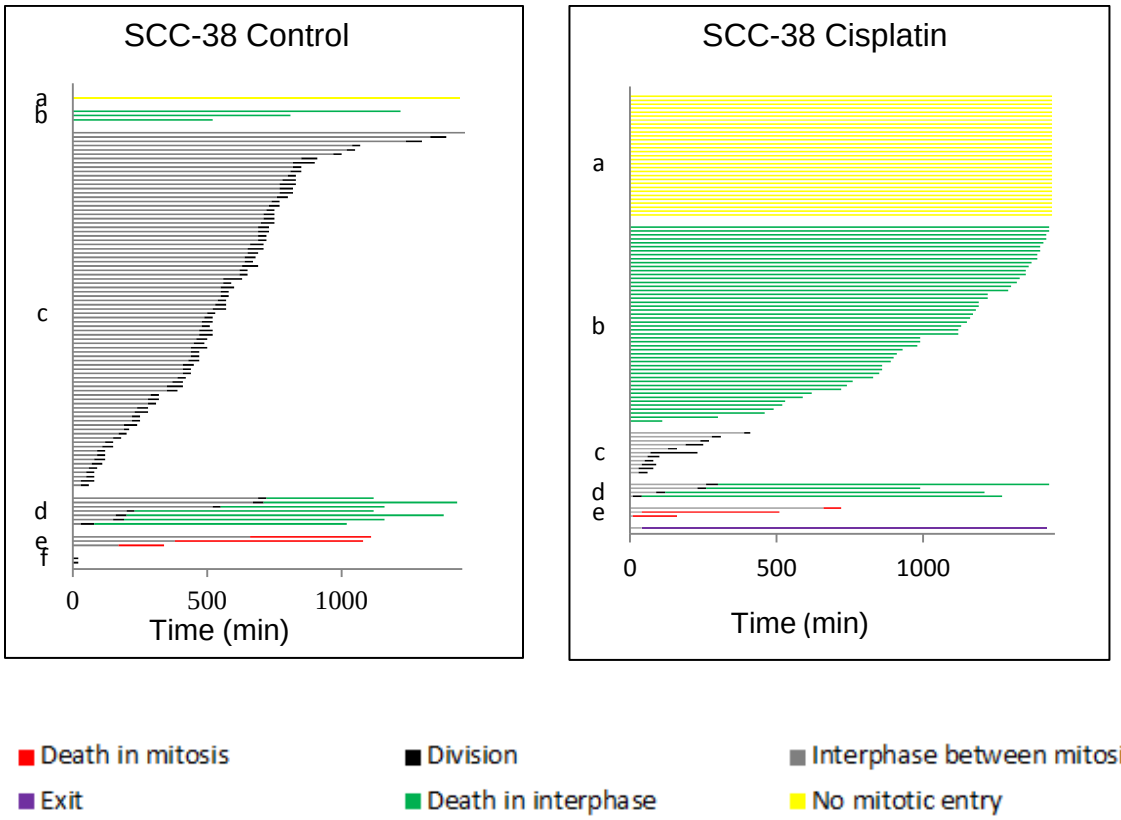

Figure 4.1.3. Diverse cell fate choices in resistant cancer cells treated with cisplatin
As described in Methods and Materials, cell fate profiles of SCC-38 cells treated with or without cisplatin were quantified. A representative experiment is shown.

Cell Behavior Distribution		
Cell behavior	**Control (%)**	**Cisplatin (%)**
a: No mitotic entry	2.4	25.4
b: Death in interphase	5.4	45.4
c: Entering mitosis and dividing	70.4	13.8
d: Entering mitosis, dividing, death in interphase	6.0	13.0
e: Entering mitosis and death in mitosis	3.6	1.2

Table 4.1. Cell behavior distribution

Table showing the percentage of SCC-38 cells in each behavioral category in the control and cisplatin treated samples. Please note: there are small percentage of cells underwent different cell fate and are not included in this table.

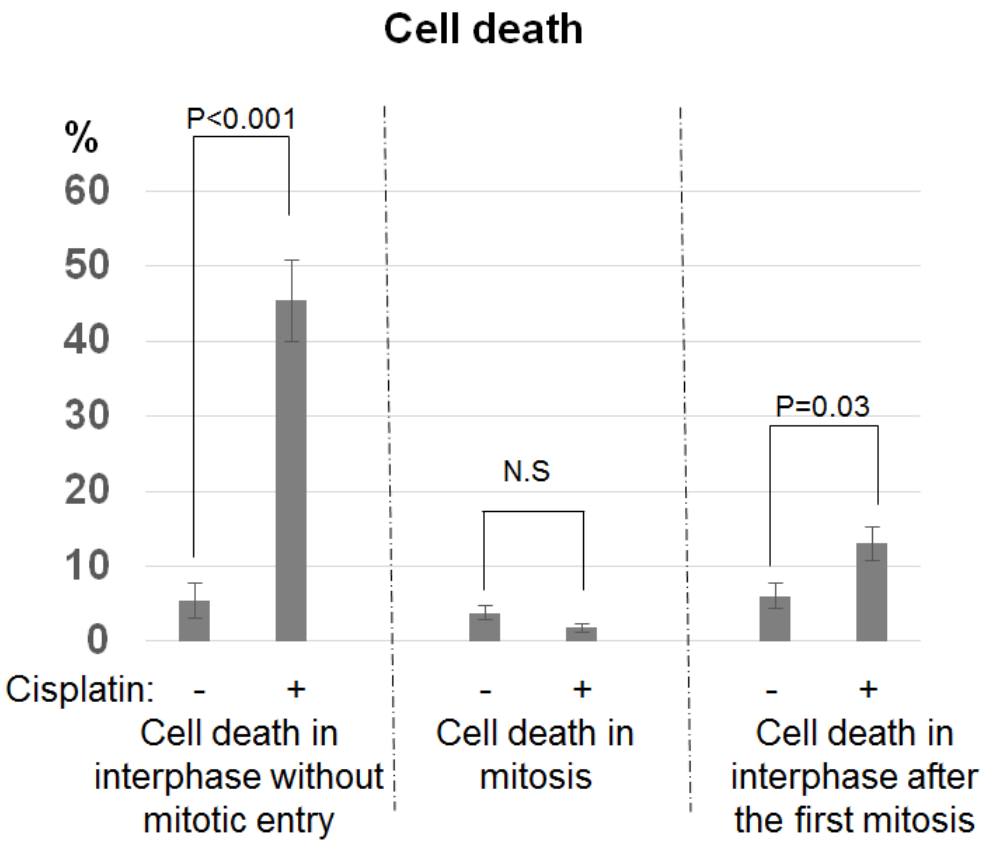

Figure 4.1.4. The induction of cell death by cisplatin in UM-SCC38 cells
The percentages of cells underwent interphase cell death without mitotic entry, death in mitosis, or in the subsequent interphase following the first mitosis were shown. SCC-38 cells without cisplatin treatment were included as a control.

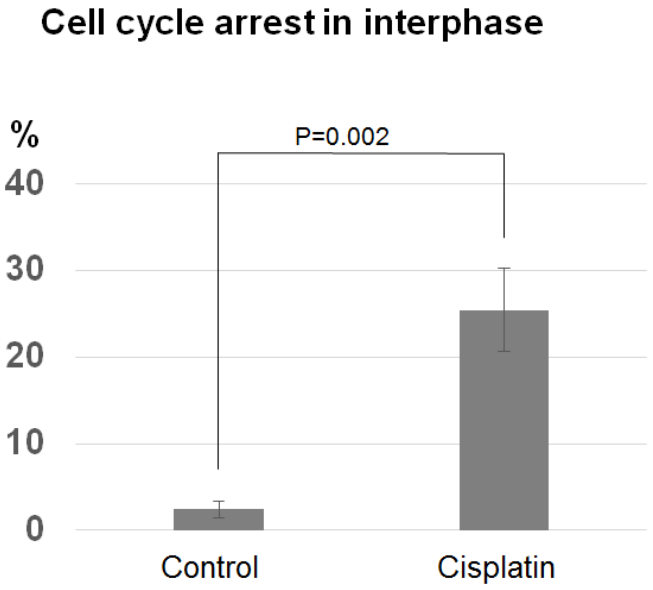

Figure 4.1.5. Cell cycle arrest in interphase
The percentages of cells that were arrested in interphase were shown in UM-SCC-38 cells with or without cisplatin.

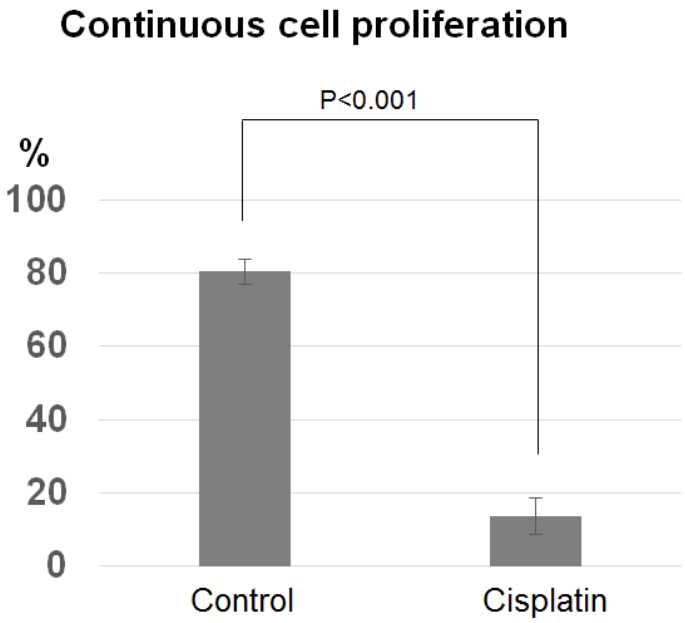

Figure 4.1.6. Continuous cell proliferation
The percentages of cell that exhibited continued cell proliferation (as judged by mitotic entry) were shown in SCC-38 cells with or without cisplatin.

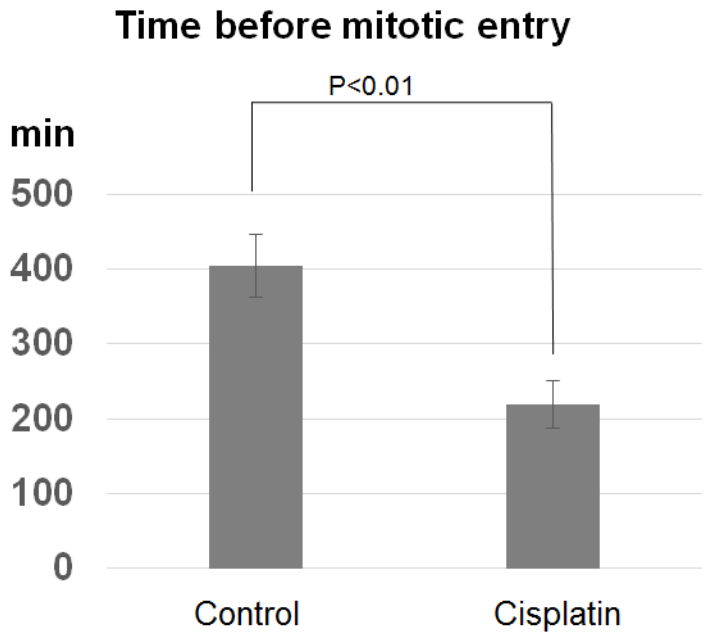

Figure 4.1.7. Time before mitotic entry
The length of interphase prior to mitotic entry was shown in the control and cisplatin-treated SCC-38 cells.

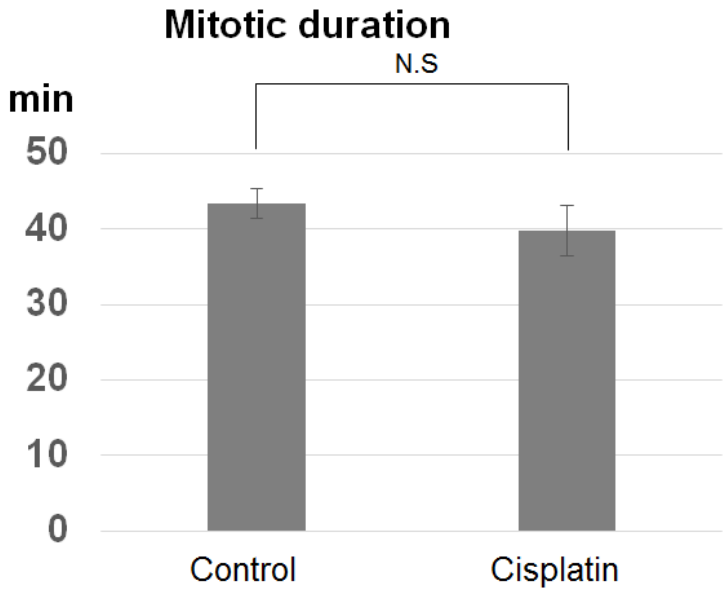

Figure 4.2.1. Mitotic duration of SCC-38 cells
The average amount of time, in minutes, that SCC-38 cells spent in mitosis when treated with or without cisplatin is shown.

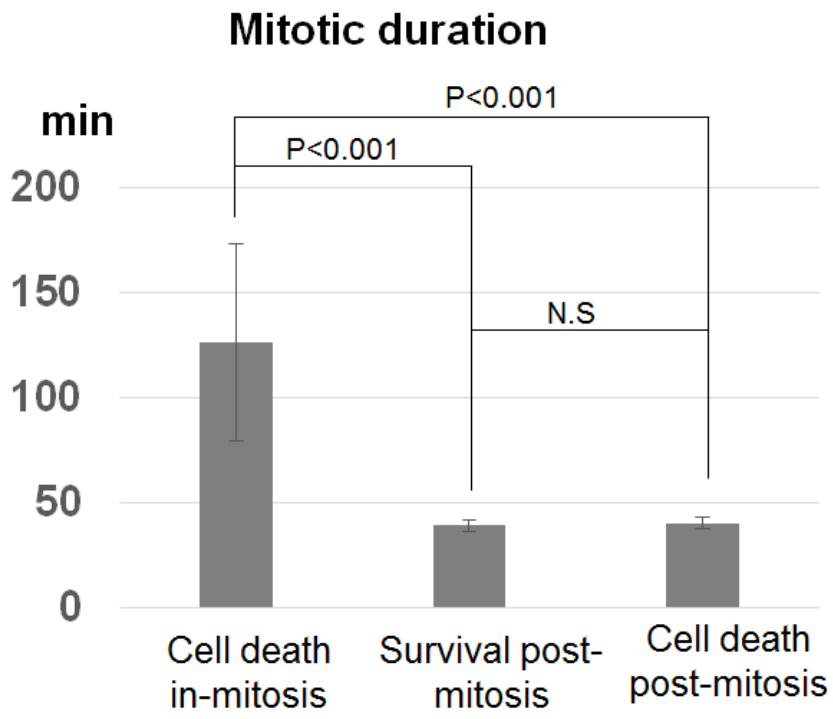

Figure 4.2.2. Mitotic duration of three post-mitotic cellular behaviors
The duration of mitotic arrest, in minutes, of three different behavioral groups of SCC-38 cells is shown.

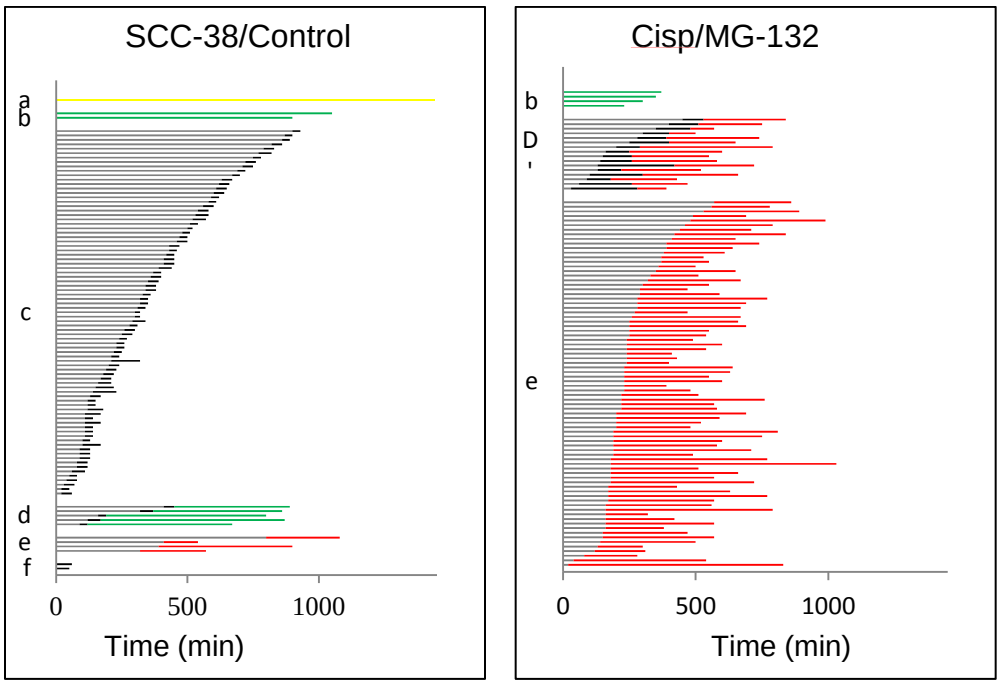

Figure 4.2.3. Cell fate choices of SCC-38 cells
Cell fate profiles of HNSCC-38 cells when treated with a combination of 16 µM cisplatin and 5 µM Mg-132

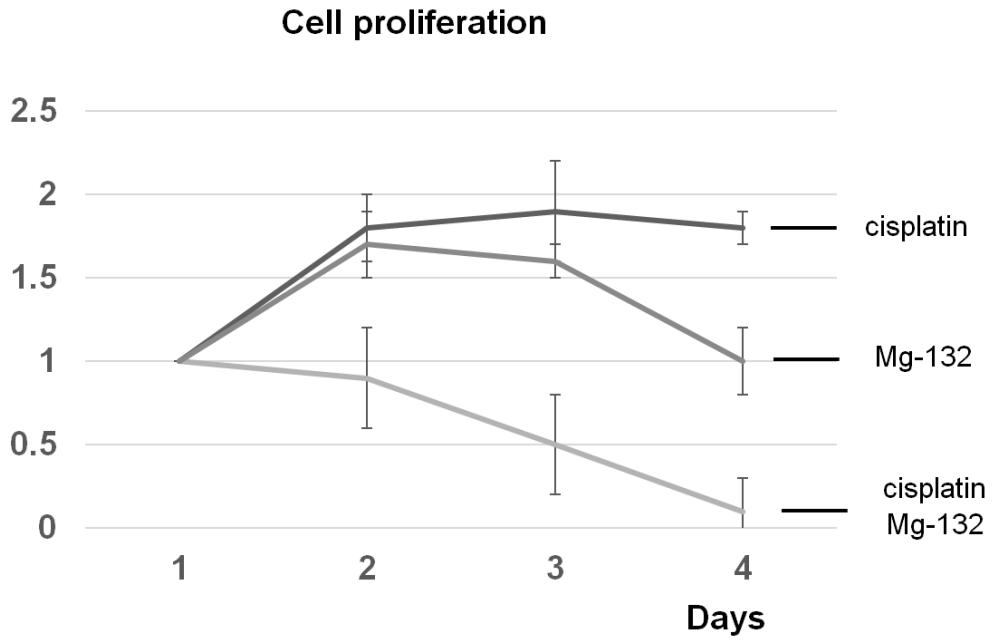

Figure 4.2.4. SCC-38 cell proliferation under the influence of drug and/or inhibitor
The SCC-38 cells were divided into three groups and subjected to cisplatin only, Mg-132 only, or cisplatin plus Mg-132 over a period of 4 days. The cell proliferation in each group was measured after each day, using hemocytometer, and the plot shows the proliferation of cells over a 4-day period. The relative cell number compared to the actual starting number on day 1 is shown.

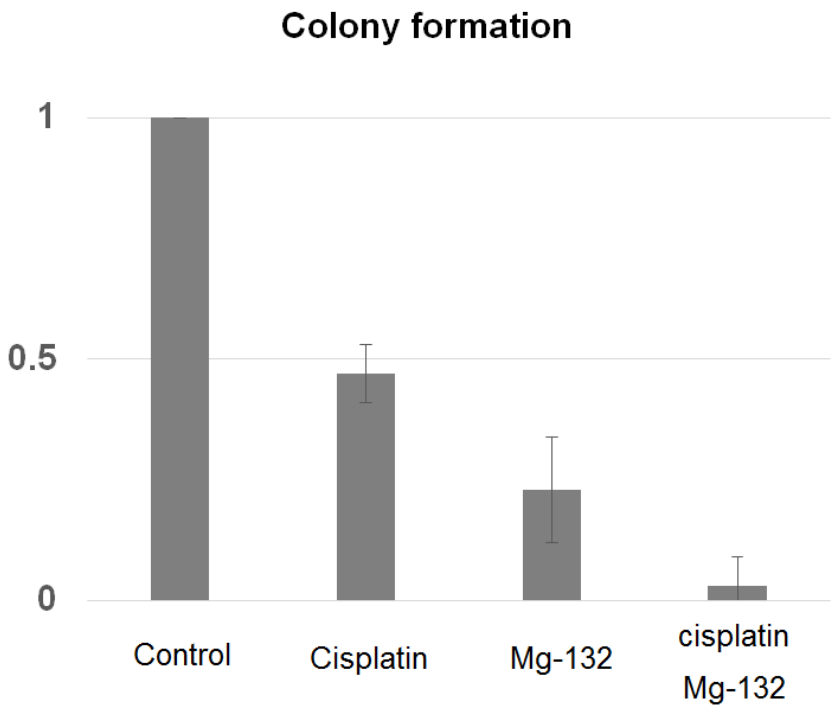

Figure 4.2.5. Cologenic assay
SCC-38 cells were untreated (control), treated with cisplatin only, Mg-132 only, or cisplatin combined with Mg-132.

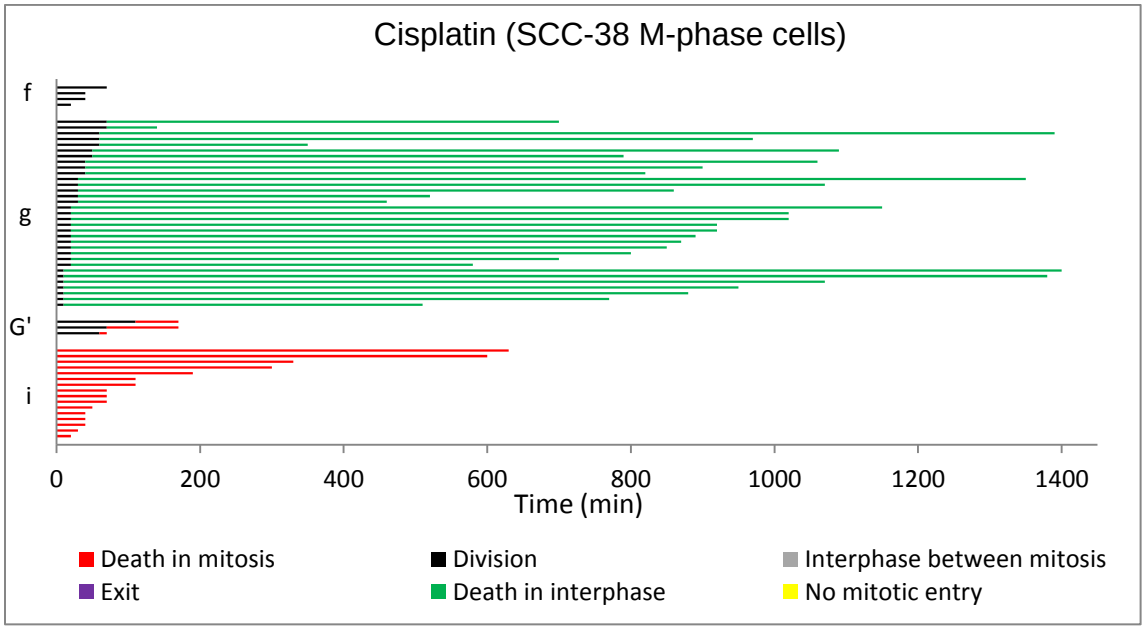

Figure 4.3.1. SCC-38 M-phase cell profile
Cell fate profiles of HNSCC-38 cells in M-phase when treated with or without cisplatin quantified and shown.

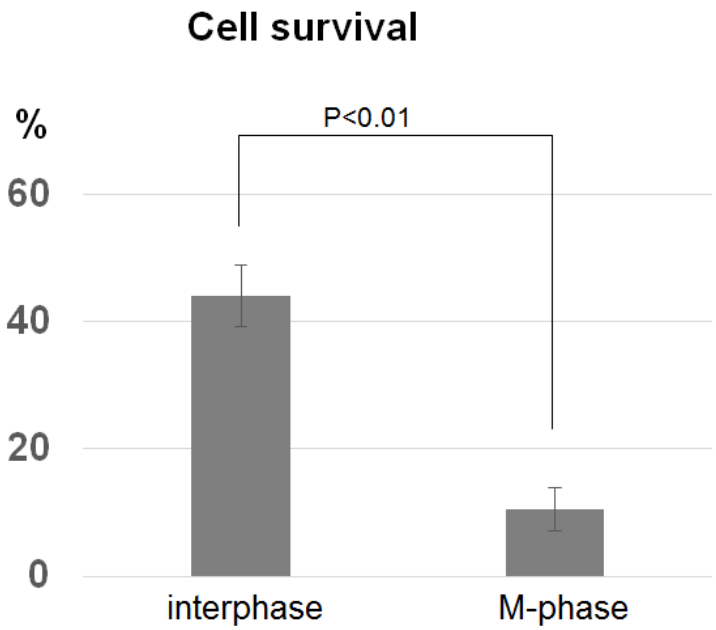

Figure 4.3.2. Asynchronized and M-phase SCC-38 cell survival
The percentages of cell survival in interphase or M-phase SCC-38 cells when treated with cisplatin.

M-phase Cell Behavior Responding to Cisplatin Treatment	
Cell Behaviors	**%**
f: Dividing during mitotic phase	7
g: Dividing and death in interphase	59
G': Dividing and death in mitosis	5
h: Interphase between mitosis	0
I: Death in mitosis	29

Table 4.3. M-phase cell behavior responding to cisplatin treatment

Table shows the distributions cell death of SCC-38 cells responding to cisplatin during M-phase.

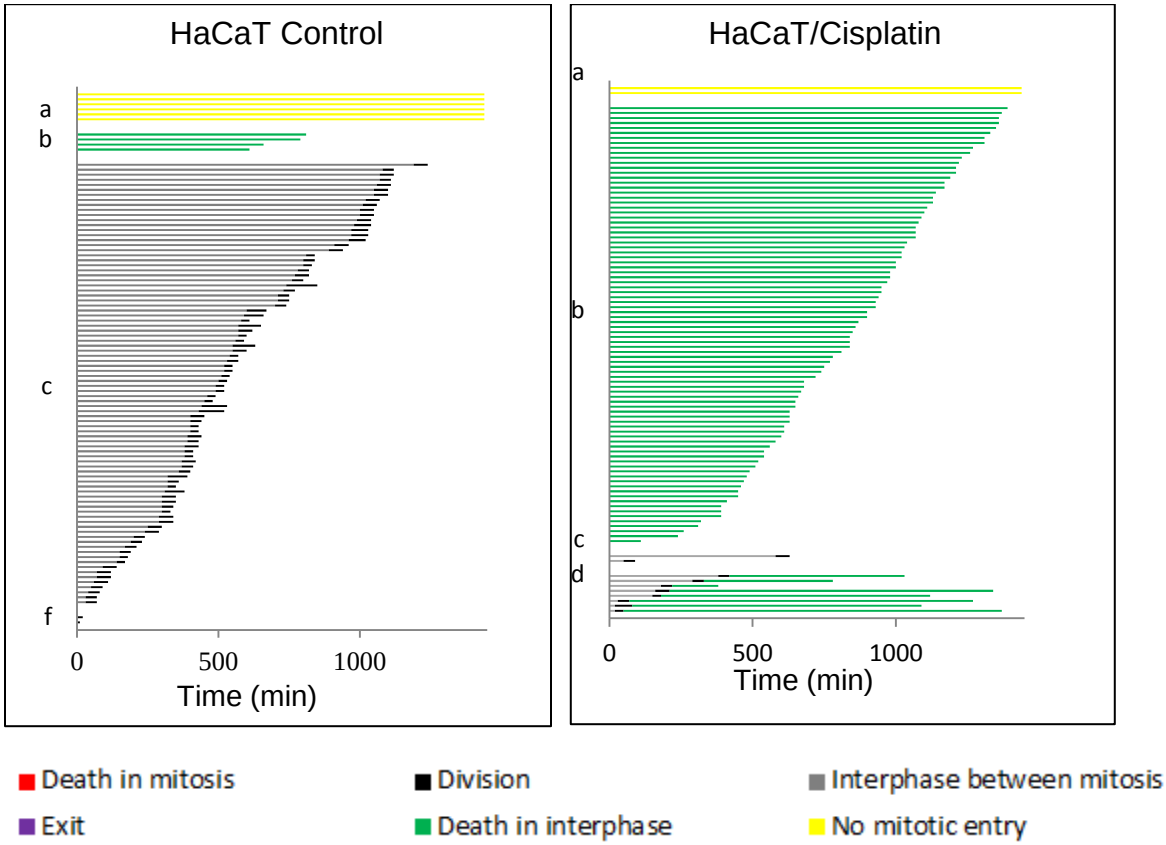

Figure 4.4.1. Cell fate profiles of HaCaT cells
Cell fate profiles of HaCaT cells treated with or without cisplatin quantified and shown. A representative experiment is shown.

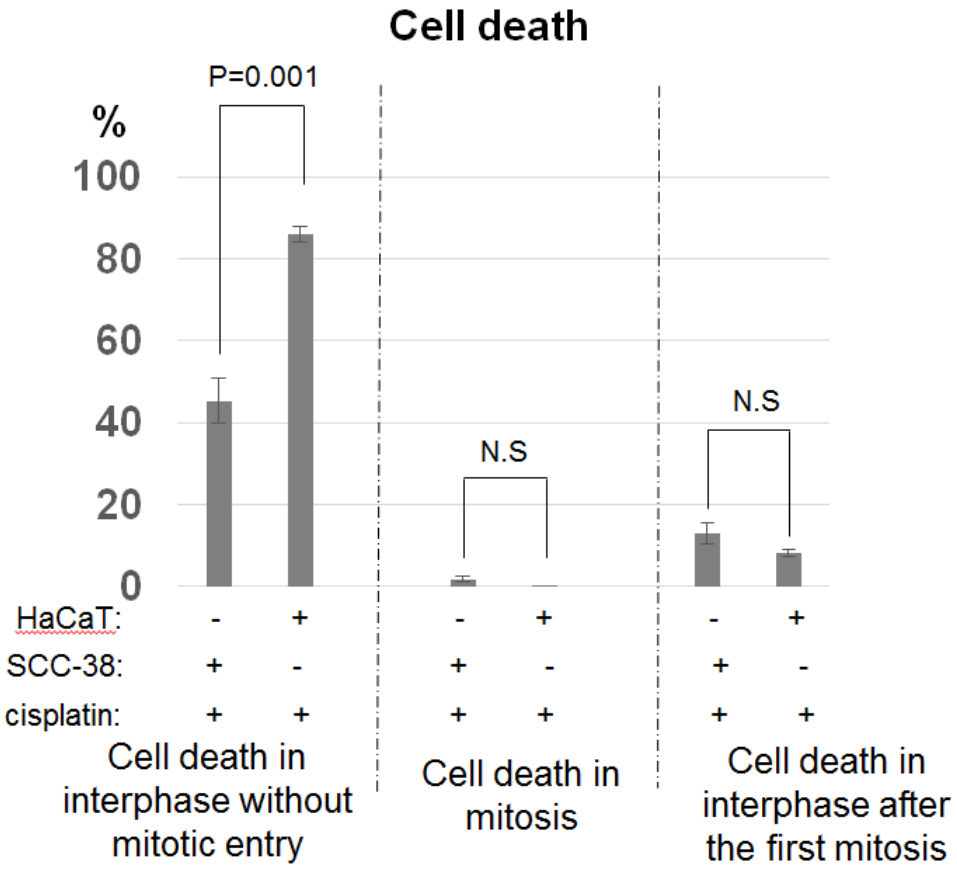

Figure 4.4.2. The induction of cell death by cisplatin in SCC-38 and HaCaT cells
The percentages of cells underwent interphase cell death without mitotic entry, death in mitosis, or in the subsequent interphase following the first mitosis were compared and shown between these two cell lines.

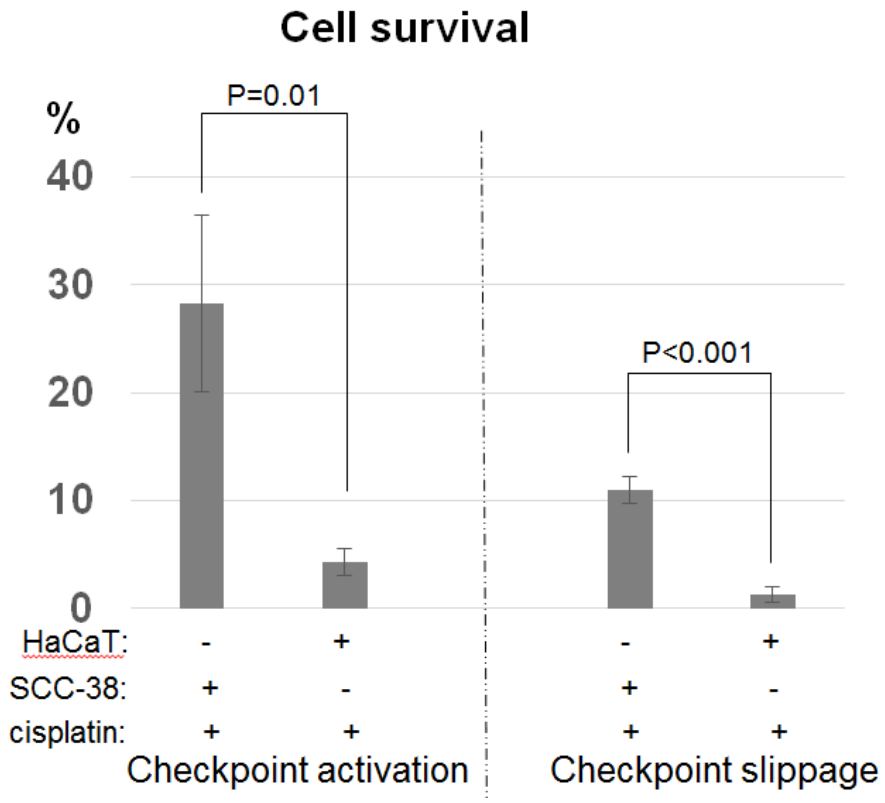

Figure 4.4.3. Cell survival via either checkpoint activation or checkpoint slippage
The percentages of HaCaT and SCC-38 cells that survived cisplatin treatment by checkpoint activation and checkpoint slippage are shown.

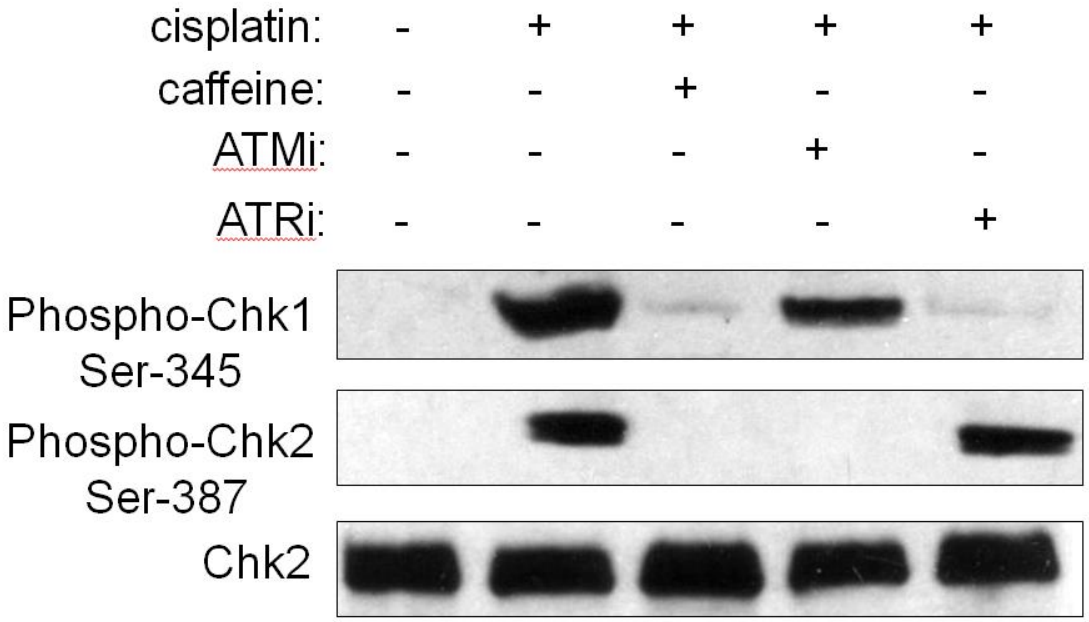

Figure 4.5.1. Western blotting
SCC-38 cells were treated with cisplatin, caffeine, and specific inhibitors of ATM and ATR (ATMi and ATRi). Phosphorylation of Chk1 and Chk2, and total Chk2 are shown by immunoblotting.

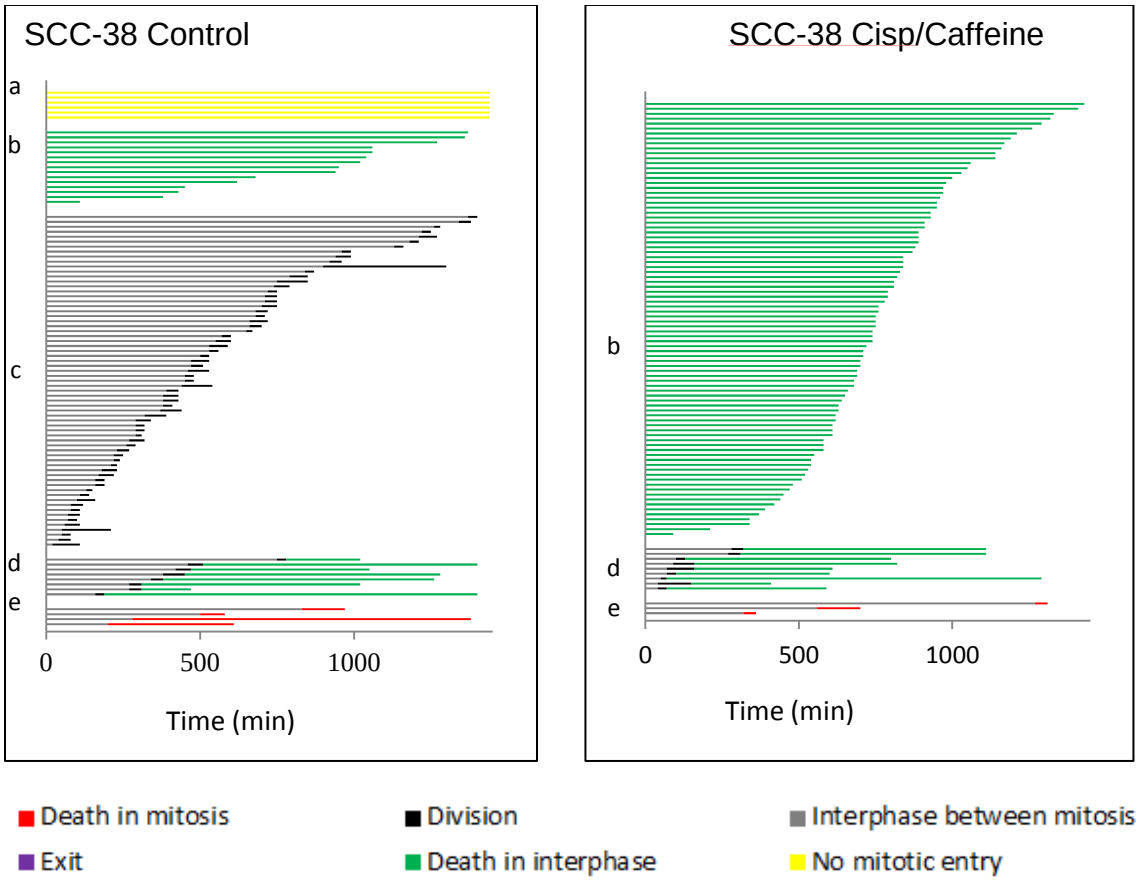

Figure 4.5.2. Cell fate choices of SCC-38 cells
Cell fate profiles of SCC-38 cells treated with cisplatin or cisplatin-caffeine combination. The concentrations for cisplatin and Mg-132 were 16µM and 5µM, respectively. A representative experiment is shown.

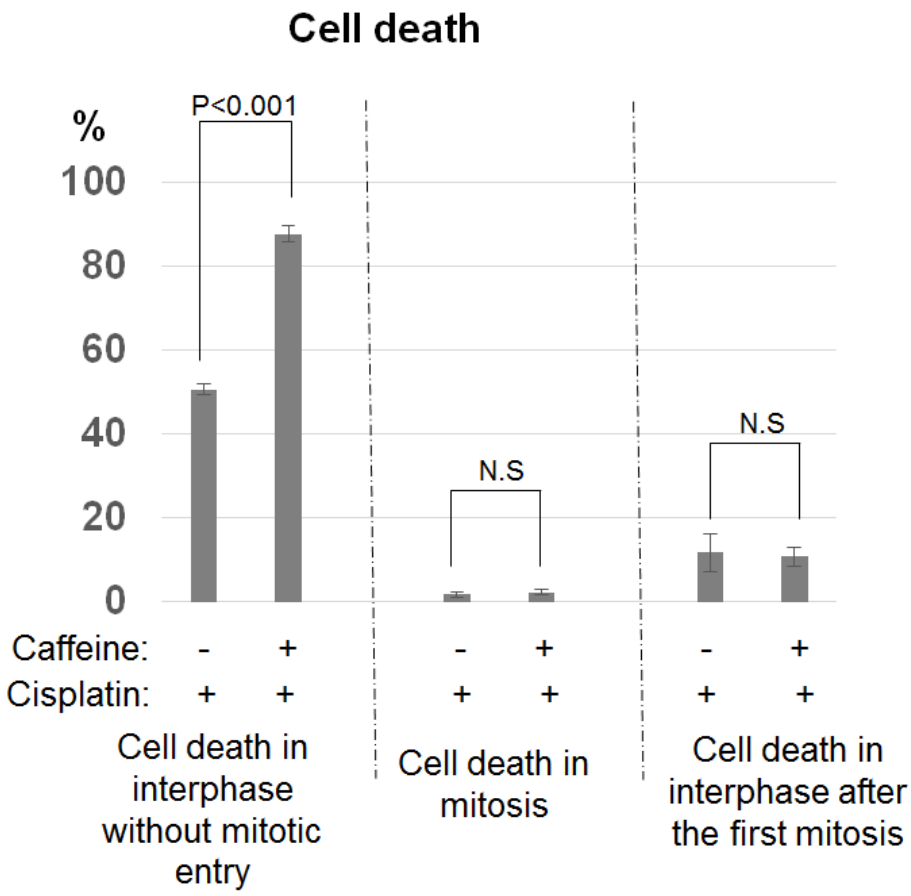

Figure 4.5.3. The induction of cell death by cisplatin plus caffeine in SCC-38 cells

The percentages of SCC-38 cells underwent interphase cell death without mitotic entry, death in mitosis, or in the subsequent interphase following the first mitosis were shown. SCC-38 cells without caffeine treatment (cisplatin only) were included to serve as comparison.

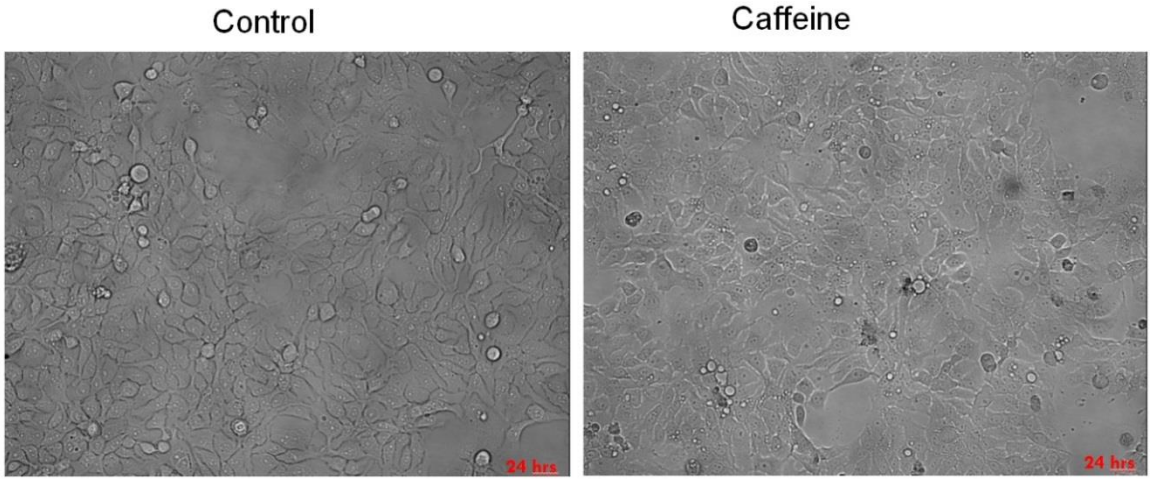

Figure 4.5.4. Light microscope photographs of SCC-38 cells
Images were taken of SCC-38 cells under the light microscope with or without caffeine treatment.
As discussed in our paper, SCC-38 cells were treated with caffeine alone to determine if caffeine had any significant behavior on cancer cells.
As evident, cell death was not significant between the two groups to warrant a time-lapse analysis.

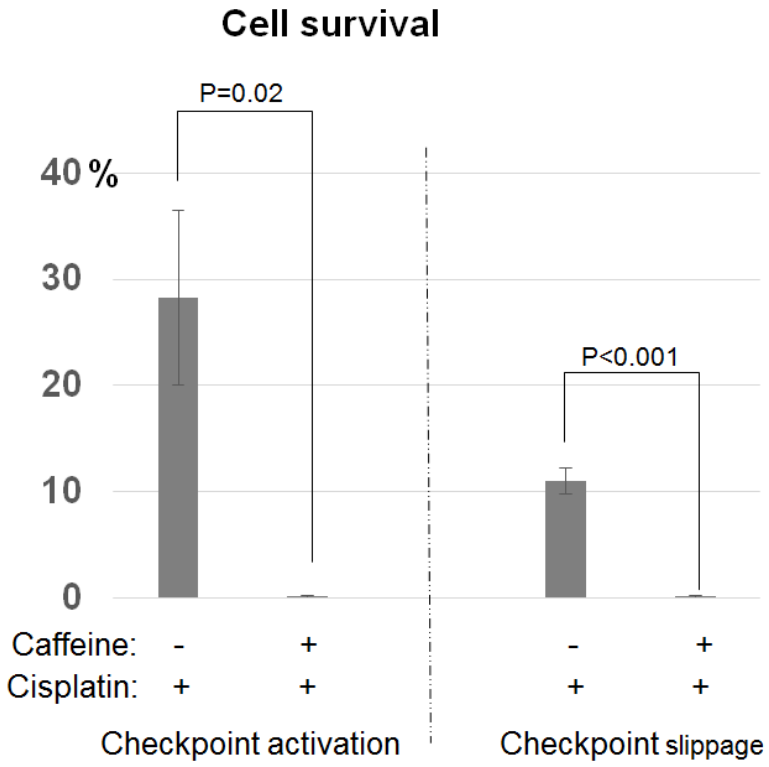

Figure 4.5.5. Cell survival via checkpoint activation or checkpoint slippage
The percentages of SCC-38 cells that survived the cisplatin plus caffeine treatment by checkpoint activation and checkpoint slippage were shown. SCC-38 cells with cisplatin only treatment were included as comparison.

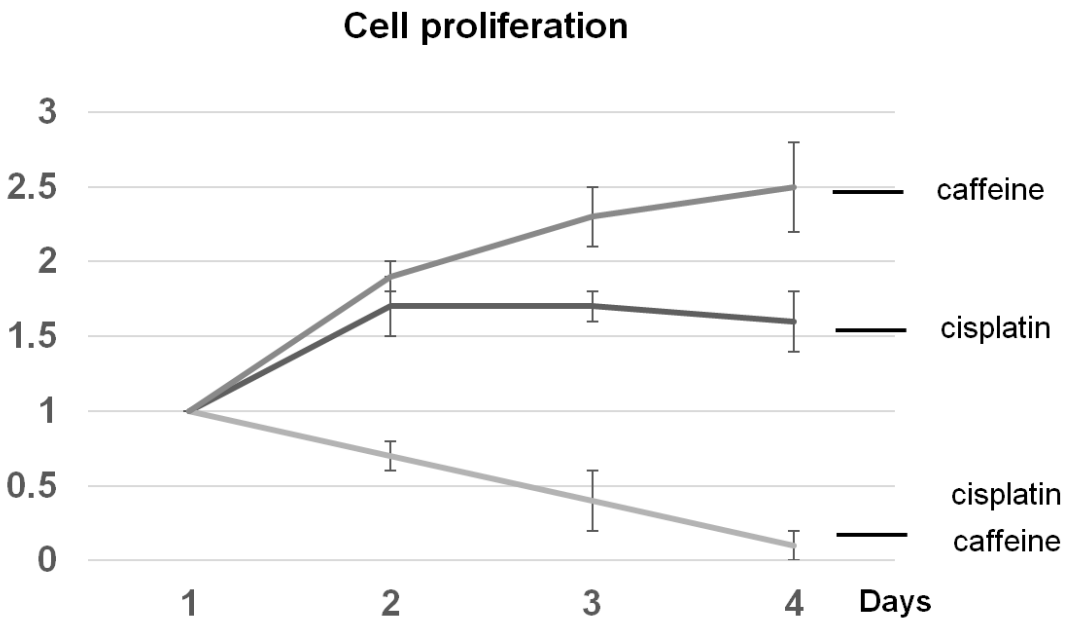

Figure 4.5.6. Cell proliferation
The SCC-38 cells were divided into three groups and subjected to cisplatin only, caffeine only, or cisplatin plus caffeine over a period of 4 days.The cell proliferation in each group was measured after each day, using hemocytometer, and the plot shows the proliferation of each group of cells over a 4-day period. The relative cell number compared to the actual starting number on day 1 is shown.

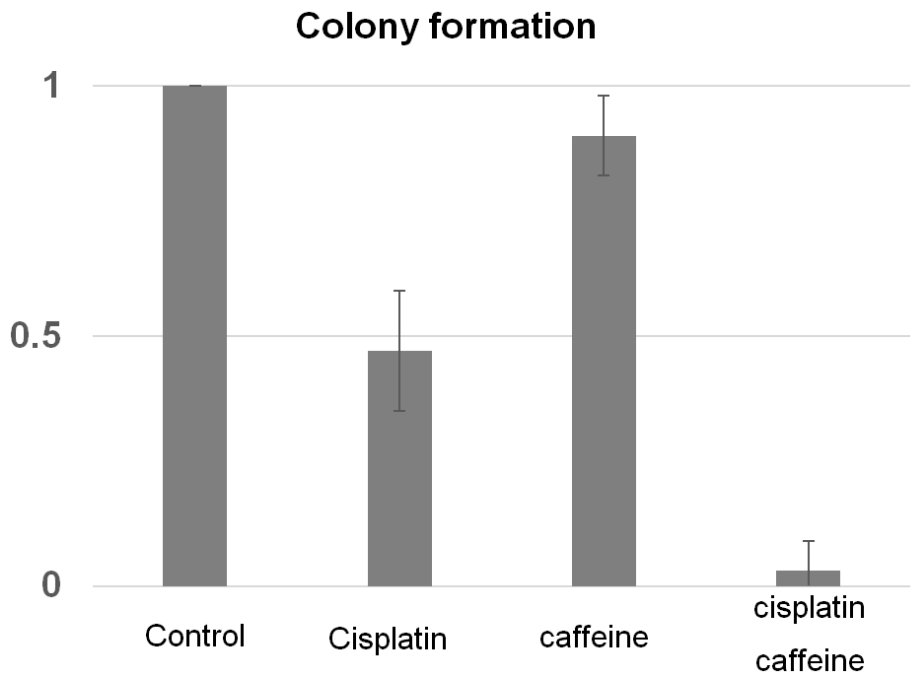

Figure 4.5.7. Clonogenic assay
SCC-38 cells were untreated (control), treated with cisplatin only, caffeine only, or cisplatin combined with caffeine.

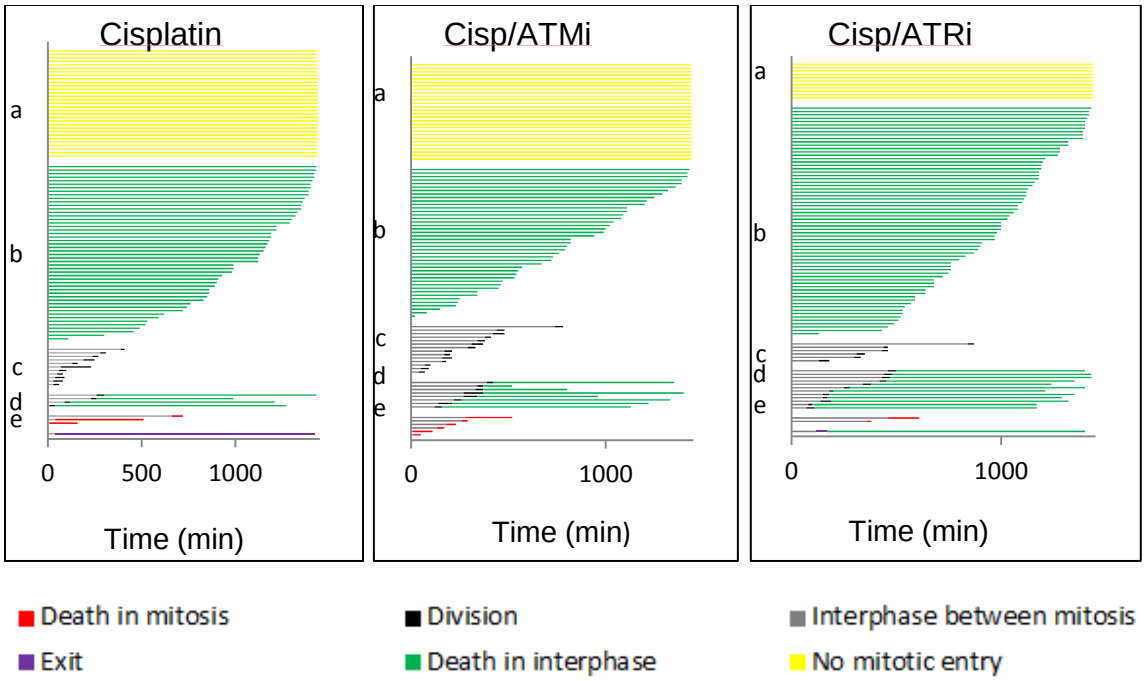

Figure 4.6.1. Inhibition of ATR, but not ATM, sensitizes the cisplatin treatment
SCC-38 cells were treated with cisplatin and ATM/ATR inhibitors as indicated. A representative experiment is shown.

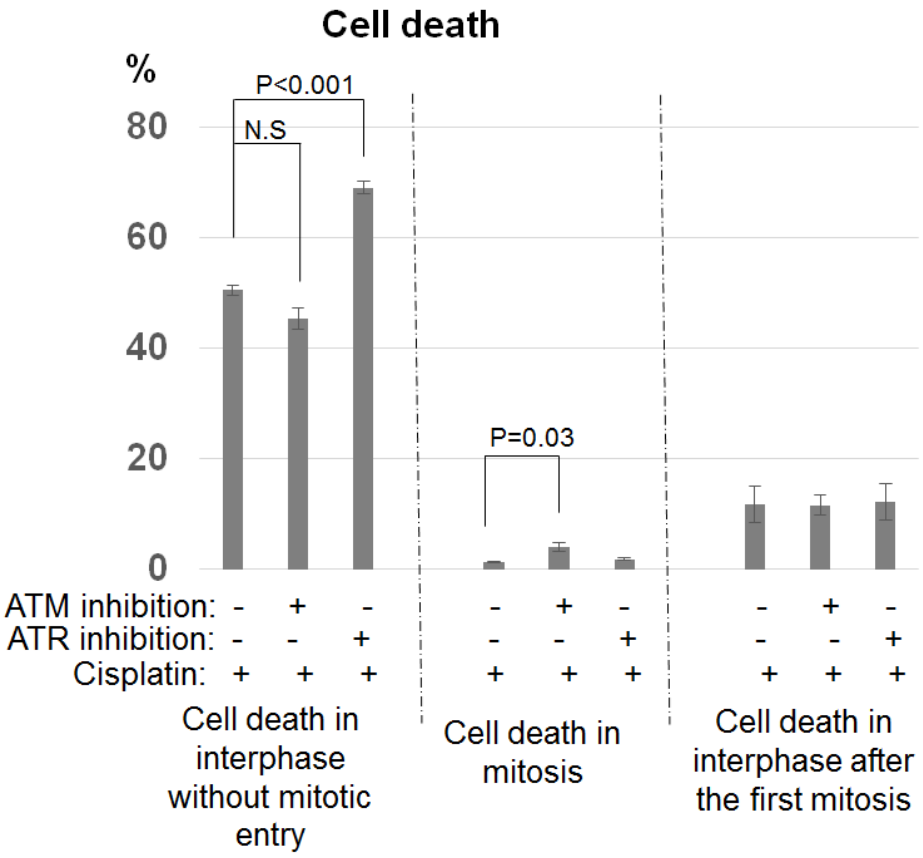

Figure 4.6.2. The induction of cell death by cisplatin and ATM/ATR inhibitors in SCC-38 cells
The percentages of cells underwent interphase cell death without mitotic entry, death in mitosis, or in the subsequent interphase following the first mitosis were shown.

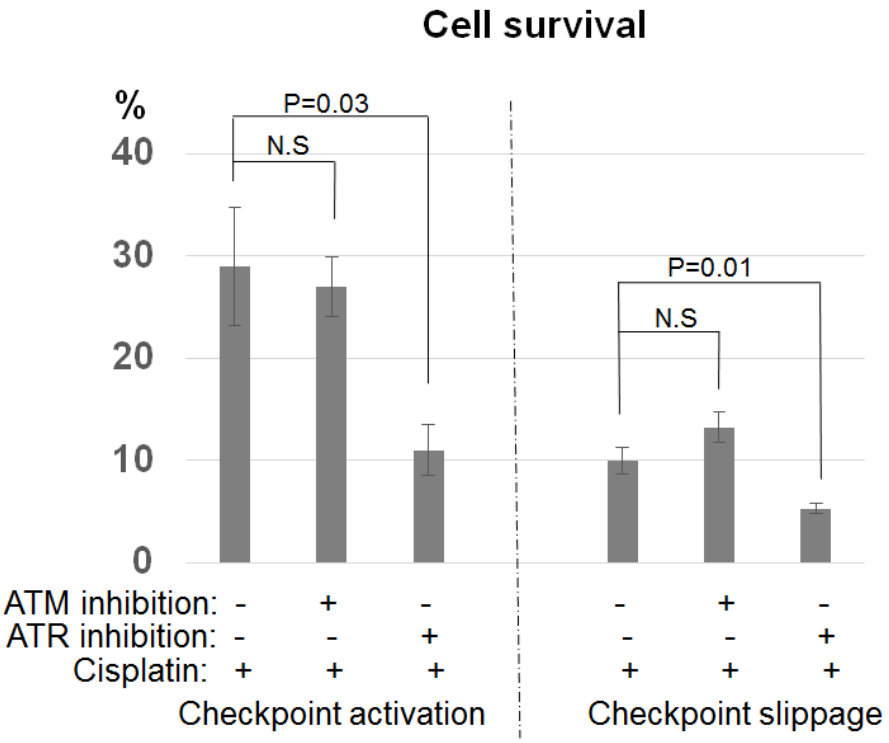

Figure 4.6.3. Cell survival via checkpoint activation or checkpoint slippage
The percentages of SCC-38 cells that survived cisplatin and ATM/ATR inhibitors by checkpoint activation and checkpoint slippage.

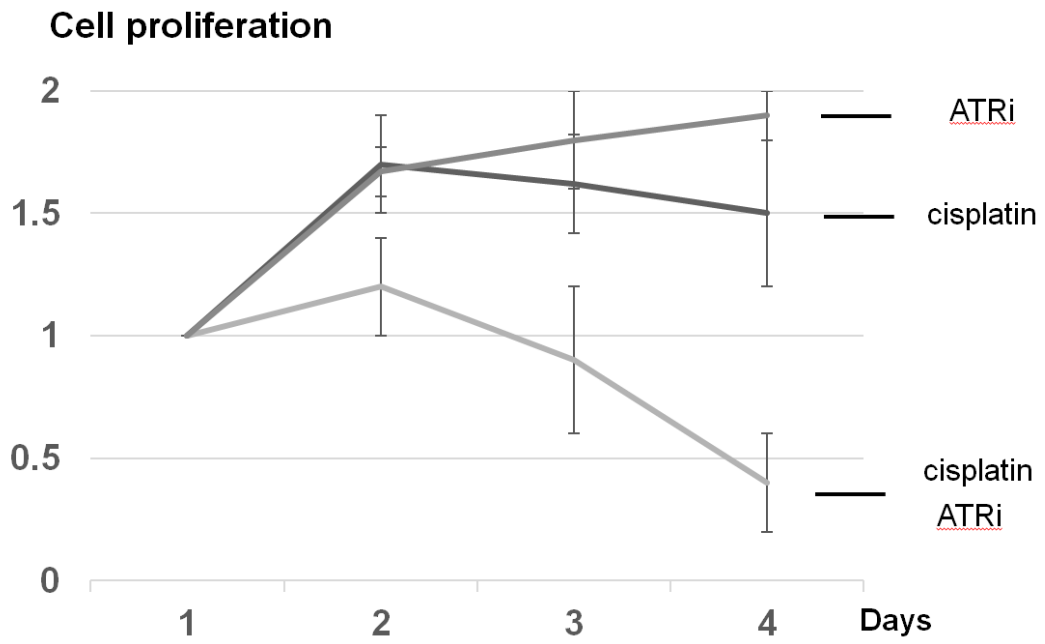

Figure 4.6.4. Cell proliferation
The SCC-38 cells were divided into three groups and subjected to cisplatin only, ATRi only, or cisplatin plus ATRi over a period of 4 days.The cell proliferation in each group was measured after each day, using hemocytometer, and the plot shows the proliferation of each group of cells over a 4-day period. The relative cell number compared to the actual starting number on day 1 is shown.

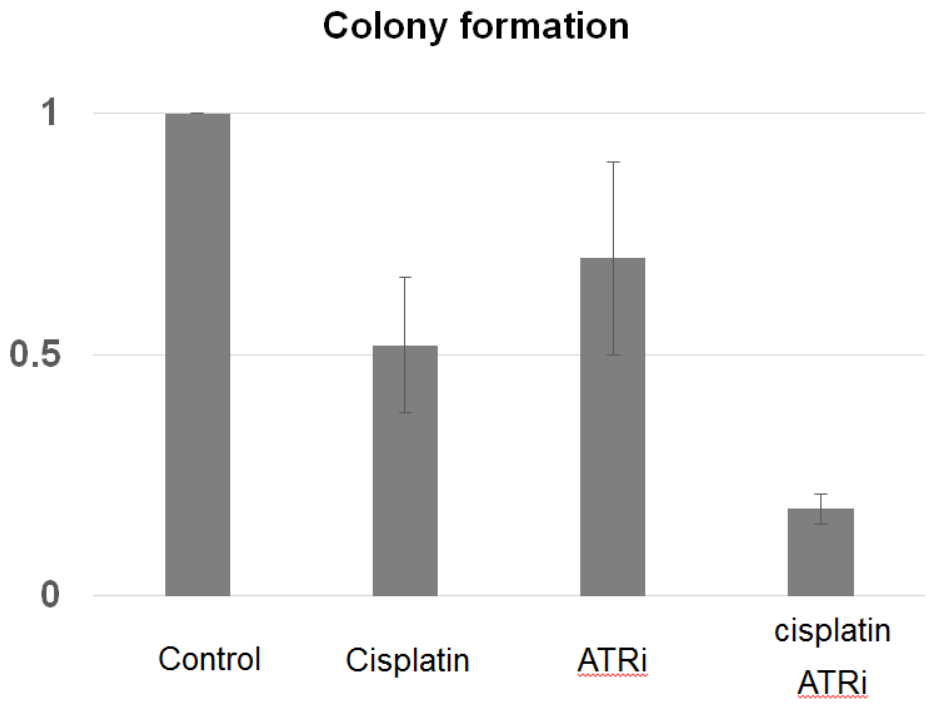

Figure 4.6.5. Clonogenic assay
SCC-38 cells were untreated (control), treated with cisplatin only, ATR inhibitor only, or cisplatin combined with ATR inhibitor.

CHAPTER 5: DISCUSSION

The ability to quantitatively measure individual cell death with live-cell imaging can reveal detailed information with respect to how cell fate choices are determined. In turn, the knowledge about cell fate choices will help us understand cancer resistance and improve treatment efficacy. In this study we profiled SCC-38 cell behavior in responding to cisplatin treatment. SCC-38 cell line was chosen due to its well-documented chemoresistance. Not surprisingly, a significantly smaller portion of SCC-38 cells died after the treatment when compared to HaCaT, a non-tumorigenic keratinocyte cell line. Interestingly, in both SCC-38 and HaCaT lines, the majority of cell death occurred in interphase without mitotic entry. By comparison, only small portions of cells either entered and then died in mitosis, or completed cell division and then died in the subsequent interphase. Analysis of the surviving SCC-38 cells revealed the co-existence of checkpoint arrest and checkpoint slippage—some surviving cells remained arrested in interphase without mitotic entry, while another group of cells underwent active cell division without detectable delay in either interphase or M-phase. Hence, our study revealed a complex pattern of cell fate choices in cancer cells treated with cisplatin.

Furthermore, we examined the length of mitosis in cells that entered mitosis after cisplatin treatment. To our surprise, cisplatin treatment did not cause prolonged mitosis, indicating the absence of vital mitotic defects or activation of the mitotic spindle checkpoint. In principle, cells entered mitosis after therapeutic treatment may die in mitosis, die after mitotic exit, or complete mitosis and survive. As

reported in this study, all these choices existed in cisplatin-treated SCC-38 cells. We then further investigated if the duration of mitosis would predict cell death or survival in the subsequent interphase. However, no significant difference was observed in the length of mitosis regardless of the cell fate after mitotic exit; as post-mitotic cell death and survival groups spent 40 and 39 minutes, respectively, in mitotic phase. Very interestingly, we found that the small portion of cisplatin-treated cells entered, and then died in mitosis typically spent more than 2 hours in mitosis prior to cell death. This association between the prolonged mitotic progression and mitotic cell death prompted us to examine the effect of delaying mitotic exit. We showed a surprisingly strong synergy between cisplatin and Mg-132, a proteasome inhibitor that was known to suppress mitotic exit. Thus, our study suggested a promising strategy of combinatorial therapy using cisplatin and Mg-132, which shall be further evaluated in laboratory or clinical studies.

Similar to interphase cells, SCC-38 cells exposed to cisplatin during mitosis exhibited diverse cell fates. However, the pattern of cell fate choices differed remarkably. Collectively, mitotic cells were more sensitive to cisplatin, and the majority of these cells died in mitosis or after mitotic exit. Thus, in addition to blocking DNA replication and transcription, our findings suggested cisplatin-induced DNA damage also interfered with mitotic progression. Moreover, recent studies showed that the molecular pathways of DNA repair and DNA damage checkpoint are largely silenced during mitosis (Heijink et al 2013; Giunta et al 2010). It has been also suggested that the mitotic suppression of DNA repair is beneficial as mitotic DNA repair may lead to chromosomal instability, e.g., via

telomere fusion (Orthwein et al 2014). Therefore, the hypersensitivity to DNA damage is a desirable choice for mitotic cells that lack the capability of DNA repair.

Since DDR plays a key role in cell fate determination after DNA damage, it has been proposed that targeting the DDR may offer a powerful tool to overcome chemoresistance. In supporting of this notion, we found that SCC-38 cells treated with caffeine, an inhibitor of ATM and ATR, exhibited greatly enhanced cell death during cisplatin treatment. Contrary to the common assumption that checkpoint disruption would lead to cell death by allowing mitotic entry with DNA damage, our study showed that caffeine-cisplatin treatment almost exclusively induced cell death in interphase without mitotic entry. As expected, caffeine suppressed checkpoint activation after cisplatin treatment, and abolished the portion of cell survival via interphase arrest. Moreover, and perhaps counterintuitively, caffeine treatment also eliminated the portion of checkpoint slippage. Therefore, we speculate that caffeine may prevent checkpoint slippage at least partially by suppressing DNA repair, as supported by several recent studies (Zelensky et al 2013; Tsabar et al 2015; Sabisz and Skladanowski 2008)

In addition to inhibit ATM and ATR simultaneously using caffeine, we further advanced the study using inhibitors that specifically target either one of these kinases. Similar to caffeine, ATR inhibition reduced cell survival by preventing checkpoint arrest and checkpoint slippage, and enhancing cell death in interphase. By comparison, ATM inhibition exhibited no significant effect on cell death or survival. Therefore, the effect of caffeine in sensitizing the cisplatin

treatment is largely conferred through ATR inhibition. However, it should be noted that the effect of ATR inhibition appeared less profound compared to that of caffeine, which implies additional targets of caffeine, as suggested previously (Cortez 2003).

CHAPTER 6: CONCLUSION

The diverse cell fate choices of SCC-38 and HaCaT cells were confirmed using live cell imaging. Our results showed the majority of cell death occurred in interphase without mitotic entry and a significantly smaller portion of SCC-38 cells died after the cisplatin treatment when compared to HaCaT. On the other hand, analysis of the surviving SCC-38 cells revealed the co-existence of checkpoint arrest and checkpoint slippage. However, caffeine was shown to abolish these surviving mechanisms in cisplatin treated cells since essentially no cells were able to survive cisplatin/caffeine treatment. Moreover, our combination therapy of cisplatin plus MG-132 showed strong synergistic effect on SCC-38 cell death. And, inhibition of ATR, instead of ATM, may be a more promising pathway to improve therapeutic outcome of cisplatin treatment. Overall, our study revealed new insights into chemoresistance and suggested combinatorial strategies that potentially overcome cancer resistance.

LITERATURE CITED

Al-Ejeh, F., et al. "Harnessing the complexity of DNA-damage response pathways to improve cancer treatment outcomes." *Oncogene* 29.46 (2010): 6085-6098.

Ashley, Amanda K., et al. "DNA-PK phosphorylation of RPA32 Ser4/Ser8 regulates replication stress checkpoint activation, fork restart, homologous recombination and mitotic catastrophe." *DNA repair* 21 (2014): 131-139.

Bartek, J., J. Bartkova, and J. Lukas. "DNA damage signalling guards against activated oncogenes and tumour progression." *Oncogene* 26.56 (2007): 7773-7779.

Bolderson, Emma, et al. "Recent advances in cancer therapy targeting proteins involved in DNA double-strand break repair." *Clinical Cancer Research* 15.20 (2009): 6314-6320.

Bode, Ann M., and Zigang Dong. "The enigmatic effects of caffeine in cell cycle and cancer." *Cancer letters* 247.1 (2007): 26-39.

Brenner, J. Chad, et al. "Genotyping of 73 UM-SCC head and neck squamous cell carcinoma cell lines." *Head & neck* 32.4 (2010): 417-426.

Caponigro, Francesco, et al. "Recent advances in head and neck cancer therapy: the role of new cytotoxic and molecular-targeted agents." *Current opinion in oncology* 18.3 (2006): 247-252.

Cortez, David. "Caffeine inhibits checkpoint responses without inhibiting the

ataxia-telangiectasia-mutated (ATM) and ATM-and Rad3-related (ATR) protein kinases." *Journal of Biological Chemistry* 278.39 (2003): 37139-37145.

Clémenson, Céline, and Marie-Claude Marsolier-Kergoat. "DNA damage checkpoint inactivation: adaptation and recovery." *DNA repair* 8.9 (2009): 1101-1109.

Crawford, Lisa JA, et al. "Comparative selectivity and specificity of the proteasome inhibitors BzLLLCOCHO, PS-341, and MG-132." *Cancer research*66.12 (2006): 6379-6386.

Deckbar, Dorothee, et al. "Chromosome breakage after G2 checkpoint release." *The Journal of cell biology* 176.6 (2007): 749-755.

Gascoigne, Karen E., and Stephen S. Taylor. "Cancer cells display profound intra-and interline variation following prolonged exposure to antimitotic drugs." *Cancer cell* 14.2 (2008): 111-122.

Giunta, Simona, Rimma Belotserkovskaya, and Stephen P. Jackson. "DNA damage signaling in response to double-strand breaks during mitosis." *The Journal of cell biology* 190.2 (2010): 197-207.

Galluzzi, L., et al., *Molecular mechanisms of cisplatin resistance.* Oncogene, 2011.

Heijink, Anne Margriet, Małgorzata Krajewska, and Marcel ATM van Vugt. "The DNA damage response during mitosis." *Mutation Research/Fundamental and Molecular Mechanisms of Mutagenesis* 750.1 (2013): 45-55.

Hurley, Paula J., and Fred Bunz. "ATM and ATR: components of an integrated

circuit." *Cell cycle* 6.4 (2007): 414-417.

Li, Yan, and Da-Qing Yang. "The ATM inhibitor KU-55933 suppresses cell proliferation and induces apoptosis by blocking Akt in cancer cells with overactivated Akt." *Molecular cancer therapeutics* 9.1 (2010): 113-125.

Lingen, M. W., et al. "Genetics/epigenetics of oral premalignancy: current status and future research*." *Oral Diseases* 17.s1 (2011): 7-22.

Lord, Christopher J., and Alan Ashworth. "The DNA damage response and cancer therapy." *Nature* 481.7381 (2012): 287-294.

Jackson, Stephen P., and Jiri Bartek. "The DNA-damage response in human biology and disease." *Nature* 461.7267 (2009): 1071-1078.

Krempler, Andrea, et al. "An imperfect G2M checkpoint contributes to chromosome instability following irradiation of S and G2 phase cells." *Cell Cycle* 6.14 (2007): 1682-1686.

Orthwein, Alexandre, et al. "Mitosis inhibits DNA double-strand break repair to guard against telomere fusions." *Science* 344.6180 (2014): 189-193.

Prevo, Remko, et al. "The novel ATR inhibitor VE-821 increases sensitivity of pancreatic cancer cells to radiation and chemotherapy." *Cancer biology & therapy* 13.11 (2012): 1072-1081.

Sabisz, M. and A. Skladanowski, *Modulation of cellular response to anticancer treatment by caffeine: inhibition of cell cycle checkpoints, DNA repair and more.* Curr Pharm Biotechnol, 2008. 9(4): p. 325-36.

Sancar, Aziz, et al. "Molecular mechanisms of mammalian DNA repair and the

DNA damage checkpoints." *Annual review of biochemistry* 73.1 (2004): 39-85.

Sanderson, Barbara JS, et al. "Mutagenic and carcinogenic properties of platinum-based anticancer drugs."*Mutation Research/Fundamental and Molecular Mechanisms of Mutagenesis*355.1 (1996): 59-70.

Shaltiel, Indra A., et al. "The same, only different–DNA damage checkpoints and their reversal throughout the cell cycle." *Journal of cell science* 128.4 (2015): 607-620.

Shiloh, Yosef. "ATM and related protein kinases: safeguarding genome integrity." *Nature Reviews Cancer* 3.3 (2003): 155-168.

Siddik, Zahid H. "Cisplatin: mode of cytotoxic action and molecular basis of resistance." *Oncogene* 22.47 (2003): 7265-7279.

Skoufias, Dimitrios A., et al. "Mitosis persists in the absence of Cdk1 activity when proteolysis or protein phosphatase activity is suppressed." *The Journal of cell biology* 179.4 (2007): 671-685.

Syljuåsen, R. G. "Checkpoint adaptation in human cells." *Oncogene* 26.40 (2007): 5833-5839.

Pabla, N., et al., *ATR-Chk2 signaling in p53 activation and DNA damage response during cisplatin-induced apoptosis.* J Biol Chem, 2008. 283(10): p. 6572-83.

Peng, Aimin. "Working hard for recovery: mitotic kinases in the DNA damage checkpoint." *Cell & bioscience* 3.1 (2013): 20.

Prendergast, A.M., et al., *Activation of DNA damage response pathways in human mesenchymal stem cells exposed to cisplatin or gamma-irradiation.* Cell Cycle, 2011. 10(21): p. 3768-77.

Teng, Pang-ning, et al. "Pharmacologic inhibition of ATR and ATM offers clinically important distinctions to enhancing platinum or radiation response in ovarian, endometrial, and cervical cancer cells." *Gynecologic oncology* 136.3 (2015): 554-561.

Toulany, Mahmoud, et al. "Cisplatin-mediated radiosensitization of non-small cell lung cancer cells is stimulated by ATM inhibition." *Radiotherapy and Oncology* 111.2 (2014): 228-236.

Tsabar, M., et al., *Caffeine impairs resection during DNA break repair by reducing the levels of nucleases Sae2 and Dna2.* Nucleic Acids Res, 2015.

Wang, Ling, et al. "Deficient DNA damage signaling leads to chemoresistance to cisplatin in oral cancer." *Molecular cancer therapeutics* 11.11 (2012): 2401-2409.

Wang, Ling, et al., *Mastl kinase, a promising therapeutic target, promotes cancer recurrence.* Oncotarget, 2014. 5(22): p. 11479-89.

Zelensky, A.N., et al., *Caffeine suppresses homologous recombination through interference with RAD51-mediated joint molecule formation.* Nucleic Acids Res, 2013. 41(13): p. 6475-89.

Zhou, Bin-Bing S., and Stephen J. Elledge. "The DNA damage response: putting checkpoints in perspective." *Nature* 408.6811 (2000): 433-439.